

**NISTIR 3977**

# **Alternating-Field Susceptometry and Magnetic Susceptibility of Superconductors**

---

---

**R. B. Goldfarb**

**M. Leental**

**C. A. Thompson**



**United States Department of Commerce**  
National Institute of Standards and Technology



# Alternating-Field Susceptometry and Magnetic Susceptibility of Superconductors

---

---

## **R. B. Goldfarb**

*National Institute of Standards and Technology  
Boulder, Colorado 80303*

## **M. Leental**

*Eastman Kodak Company  
Rochester, New York 14650*

## **C. A. Thompson**

*National Institute of Standards and Technology  
Boulder, Colorado 80303*

October 1991

### *Presented at:*

Office of Naval Research Workshop on  
Magnetic Susceptibility of Superconductors and Other Spin Systems,  
Berkeley Springs, West Virginia,  
20 May 1991

### *Published in:*

"Magnetic Susceptibility of Superconductors and Other Spin Systems,"  
R. A. Hein, T. L. Francavilla, and D. H. Liebenberg, Editors,  
Plenum Press, New York (1992)





# ALTERNATING-FIELD SUSCEPTOMETRY AND MAGNETIC SUSCEPTIBILITY OF SUPERCONDUCTORS

**R. B. Goldfarb**

*National Institute of Standards and Technology  
Boulder, Colorado 80303*

**M. Lelental**

*Eastman Kodak Company  
Rochester, New York 14650*

**C. A. Thompson**

*National Institute of Standards and Technology  
Boulder, Colorado 80303*

## ABSTRACT

This review critically analyzes current practice in the design, calibration, sensitivity determination, and operation of alternating-field susceptometers, and examines applications in magnetic susceptibility measurements of superconductors. Critical parameters of the intrinsic and coupling components of granular superconductors may be deduced from magnetic susceptibility measurements. The onset of intrinsic diamagnetism corresponds to the initial decrease in electrical resistivity upon cooling, but the onset of intergranular coupling coincides with the temperature for zero resistivity. The lower critical field may be determined by the field at which the imaginary part of susceptibility increases from zero. Unusual features in the susceptibility of superconductor films, such as a magnetic moment that is independent of film thickness and the variation of susceptibility with angle, are related to demagnetization. Demagnetizing factors of superconductor cylinders are significantly different from those commonly tabulated for materials with small susceptibilities. Rules for the susceptibility of mixtures with specific demagnetizing factors are used to estimate the volume fraction of superconducting grains in sintered materials. Common misunderstandings of the Meissner effect, magnetic units, and formula conversions are discussed. There is a comprehensive summary of critical-state formulas for slabs and cylinders, including new equations for complex susceptibility in large alternating fields. Limitations on the use of the critical-state model for deducing critical current density are listed and the meaning of the imaginary part of susceptibility is considered.

## INTRODUCTION

The term “susceptibility” was originated by William Thomson (Lord Kelvin) in his annotated *Reprint of Papers on Electrostatics and Magnetism*.<sup>1</sup> He defined “the magnetic susceptibility of an isotropic substance [as] the intensity of magnetization acquired by an infinitely thin bar of it placed lengthwise in a uniform field of unit magnetic force.” The specification of an infinitely thin bar eliminated the need to consider demagnetizing fields. The stipulation of a field of unit magnetic force defined susceptibility as the ratio of magnetization  $M$  (magnetic moment per unit volume) to magnetic field strength  $H$ . Thomson distinguished between susceptibility<sup>2</sup> and permeability, a term he devised to mean the ratio of magnetic induction  $B$  to  $H$ .

Magnetization and susceptibility measurements on superconductors detect signals, usually inductively, that have their origins in circulating persistent shielding currents, in addition to any magnetic properties of the material. We distinguish between eddy currents in normal metals, which decay with time, and shielding currents in superconductors, which do not. Susceptibility may be measured using direct or alternating magnetic fields, yielding the ac susceptibility or the dc susceptibility. For either, we define  $\chi$  as the differential magnetic susceptibility  $dM/dH$ ; we do not necessarily require that  $dH \rightarrow 0$ . In dc susceptibility, the zero-field-cooled (ZFC) curve demonstrates flux shielding (flux exclusion) upon warming, and the field-cooled (FC) curve demonstrates the Meissner effect (flux expulsion) upon cooling. Whether measured upon warming or cooling, ac susceptibility (with no dc bias field) always measures shielding.

It is easier to define a superconductor as a material with zero electrical resistivity than it is to experimentally verify zero resistivity. A four-point measurement of resistivity involves the selection of current, voltage criterion, correction for thermoelectric voltages, contact geometry, and the effect of magnetic field, including the self-field of the current. The magnetic manifestation of zero resistivity is that a material is a superconductor if it exhibits perfect diamagnetic shielding; that is, its susceptibility  $\chi$  is exactly  $-1$  (in SI units, where numerical results must be corrected for any sample demagnetizing factor). Susceptibility is reminiscent of electrical conductivity  $\sigma$ , both functions of temperature  $T$ :  $\chi(T)/\chi(0) \approx \sigma(T)/\sigma(0)$ . In the normal state, both are small. In the superconducting state, both are large. Important variables are the magnitude of the measuring field and the definition of the critical temperature  $T_c$  in terms of the onset, midpoint, or end of the diamagnetic transition.

## MEISSNER EFFECT

The Meissner-Ochsenfeld effect<sup>3</sup> is the expulsion of magnetic flux upon cooling a superconductor through  $T_c$  in a dc magnetic field or upon reducing the magnetic field through the upper critical field  $H_{c2}$  at constant temperature. Type-II superconductors will not exhibit a pronounced Meissner effect if they have good flux pinning (important for high critical current density  $J_c$ ) in the mixed state. Thus, while a material that has a Meissner effect is a superconductor, the converse is not necessarily true. What is

sometimes called the “Meissner state” in superconductors is better termed the shielding state, perfect diamagnetism.<sup>4</sup>

It has long been known that the Meissner effect is incomplete in many materials. Shoenberg stated that “for many of the element superconductors, it has not yet been possible to obtain a specimen which shows a complete Meissner effect....”<sup>5</sup> Tantalum, a type-I superconductor, is a case in point, with a Meissner effect of only 1%.<sup>6</sup> Shoenberg attributed the incomplete Meissner effect in tantalum to its “mechanical state rather than ... chemical impurities.”<sup>7</sup> Years later, Alers *et al.* returned to this: “It is well known that for tantalum the Meissner effect is practically nonexistent because the metal freezes in all of the existing flux when it becomes superconducting.... Pure tantalum in bulk ... [is] made by sintering ... small flakes or grains.... Thus from a physical point of view, the metal is not homogeneous, and one can understand that the Meissner effect might not be realized by a metal of this physical make up.”<sup>8</sup> The similarity between the morphologies of sintered tantalum and sintered Y–Ba–Cu–O (or any of its analogs) will not be lost on most readers. However, sintered materials are not unique in this respect. Type-II elements and alloys and other inhomogeneous superconductors,<sup>5,6,9</sup> including *melt-cast* tantalum,<sup>10</sup> similarly fail to show a significant Meissner effect. The Meissner effect is also incomplete in *single crystals* of  $\text{YBa}_2\text{Cu}_3\text{O}_{7-\delta}$ , which suggests intragrain pinning sites.<sup>11</sup>

It is experimentally found that, in weak fields, the Meissner effect approaches 100%,<sup>11–15</sup> a value defined by the ZFC susceptibility curve. This is not surprising; it is tautologous that FC *upon warming* is equivalent to ZFC when the measuring field is zero. If the FC curve were completely reversible for warming and cooling in the limit of zero field, the Meissner effect would of necessity approach 100%.

## CRITICAL TEMPERATURE

In field–current-density–temperature ( $H$ – $J$ – $T$ ) space, there is a critical surface, with axis intercepts  $H_c$ ,  $J_c$ , and  $T_c$ , separating the superconducting and normal states. Its intersection with the  $H$ – $T$  plane may be regarded as  $H_c$  versus  $T$  or  $T_c$  versus  $H$ , and similarly for intersections with the  $J$ – $T$  and  $J$ – $H$  planes. For type-II superconductors the  $H$ -axis intercept is the upper critical field  $H_{c2}$ . The mixed state lies between  $H_{c2}$  and the lower critical field  $H_{c1}$ .

Measured as functions of temperature, transitions in resistivity  $\rho$  and susceptibility  $\chi$  may be used to define  $T_c$ . Ideally,  $T_c$  should be determined at  $J = 0$  and  $H = 0$ . However, measurements of  $\rho$  require some  $J$  and measurements of  $\chi$  require some  $H$ . These are best kept small, unless the current and field dependences are specifically required. Electrical resistivity complements susceptibility. Resistivity is a one-dimensional measurement. A specimen will show zero resistivity if there is a single zero-resistance percolation path. A higher- $T_c$  phase can mask the presence of a lower- $T_c$  phase. Either of these cases could lead to erroneous conclusions regarding the microstructure of the specimen under study. Susceptibility is a two-dimensional measurement in the sense that a surface current sheath is required for full

diamagnetism. The interior of the material could remain normal or have a lower  $T_c$ . Both measurements deceive because they do not probe the entire sample volume. "Onset" temperatures (defined as *onset upon cooling*, even if the measurement is made upon warming) occur with the first zero-resistance segment and the first zero-resistance current circuit, for  $\rho$  and  $\chi$  respectively. In low-dimensional systems, fluctuation effects may obscure the onset of superconductivity.<sup>16</sup>

### *Granular and Multifilamentary Superconductors*

Sintered high- $T_c$  superconductors and composite low- $T_c$  superconductors with closely spaced filaments exhibit two critical temperatures. One is intrinsic to the superconductor and the other is characteristic of the coupling between either grains<sup>9,17-25</sup> or filaments.<sup>26</sup> In such materials, the coupling component supports supercurrents and has its own effective  $T_c$ ,  $J_c$ ,  $H_{c1}$ , and  $H_{c2}$ . In multifilamentary niobium-titanium (Nb-Ti) and niobium-stannide (Nb<sub>3</sub>Sn) superconductors, the coupling component is the normal-metal matrix and the coupling mechanism is the proximity effect.<sup>26-29</sup> The situation is less certain in sintered high- $T_c$  compounds, but lack of stoichiometry at the grain boundaries could give rise to normal metal barriers<sup>30-32</sup> and proximity-effect coupling.<sup>33-36</sup> Another coupling mechanism in sintered materials is microbridges between grains.<sup>37</sup> Low-dimensional compounds, such as Nb<sub>3</sub>Se<sub>4</sub>, exhibit coupling attributed to superconductor-insulator-superconductor Josephson junctions.<sup>38</sup>

Because of the large change in shielded volume that occurs at  $T_c$  of the coupling component, there is a striking change in susceptibility. The change in resistivity, in comparison, is minor because the coupling component forms a small part of the conduction path. A crushed sintered sample yields isolated grains with only intrinsic characteristics.<sup>18,24,25,35,39,40</sup> Both intrinsic and coupling critical temperatures are

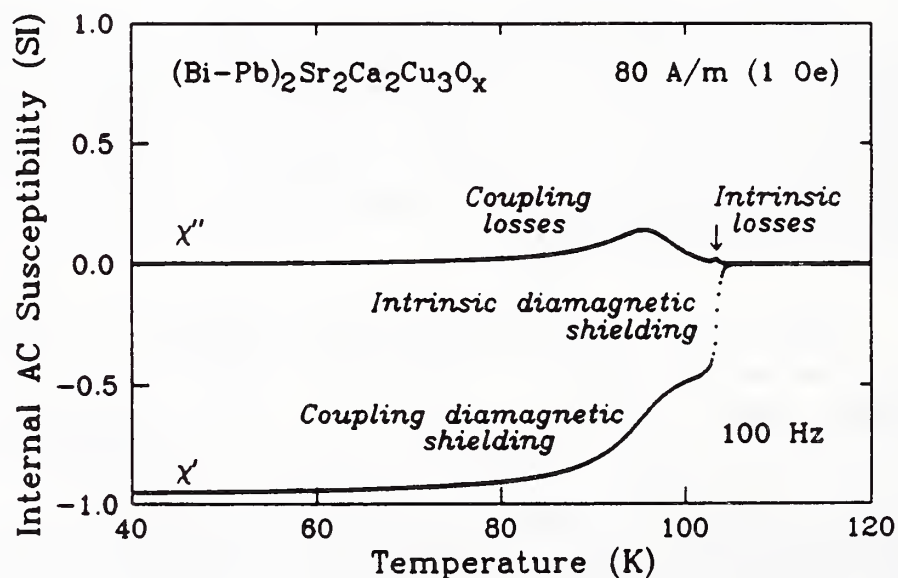


Fig. 1. Internal ac susceptibility for  $(\text{Bi-Pb})_2\text{Sr}_2\text{Ca}_2\text{Cu}_3\text{O}_x$ . The measurement field,  $80 \text{ A} \cdot \text{m}^{-1}$  rms at 100 Hz, is large enough to separate the intrinsic and coupling components. The real part does not extrapolate to  $-1$  because the demagnetizing factor used to reduce the data was approximate.

field dependent, the latter more so.<sup>17,19,23,40</sup> This dependence may be examined with increasing ac measurement fields or dc bias fields.<sup>41</sup>

For high quality, strongly coupled, sintered superconductors, the two critical temperatures coincide for small measuring fields.<sup>17</sup> The coupling  $T_c$  is not depressed as much with increasing measurement field compared to a poor quality, weakly coupled sample. A typical measurement<sup>42</sup> for a sample of high quality, sintered, high- $T_c$   $(\text{Bi-Pb})_2\text{Sr}_2\text{Ca}_2\text{Cu}_3\text{O}_x$  is presented in Fig. 1. The real ( $\chi'$ ) and imaginary ( $\chi''$ ) parts of internal susceptibility (corrected for demagnetizing factor) are shown as a function of increasing temperature, with the intrinsic and coupling segments identified. The measurement field of  $80 \text{ A}\cdot\text{m}^{-1}$  rms is large enough to separate the two components. For a small measurement field of  $0.8 \text{ A}\cdot\text{m}^{-1}$  rms, the critical temperatures overlap.

Figure 2 shows internal ac susceptibility curves for poor quality, weakly coupled, sintered  $\text{YBa}_2\text{Cu}_3\text{O}_{7-\delta}$  measured in  $0.8 \text{ A}\cdot\text{m}^{-1}$  and  $80 \text{ A}\cdot\text{m}^{-1}$  rms. Even for the lower measurement field, the coupling  $T_c$  ( $90.3 \text{ K}$ ) is considerably below the intrinsic  $T_c$  ( $91.1 \text{ K}$ ). There is no intrinsic  $\chi''$  peak for this sample for the fields used.

### Identification of Critical Temperature

In resistivity measurements,  $T_c$  is the temperature at which a percolation path is established. The corresponding temperature for magnetic susceptibility occurs when a bulk shielding path is established. This occurs at  $T_c$  of the coupling component, in particular at the onset of coupling. The distinction between the intrinsic onset and coupling onset is pertinent for samples with weak coupling and for measurements made in moderately large fields.

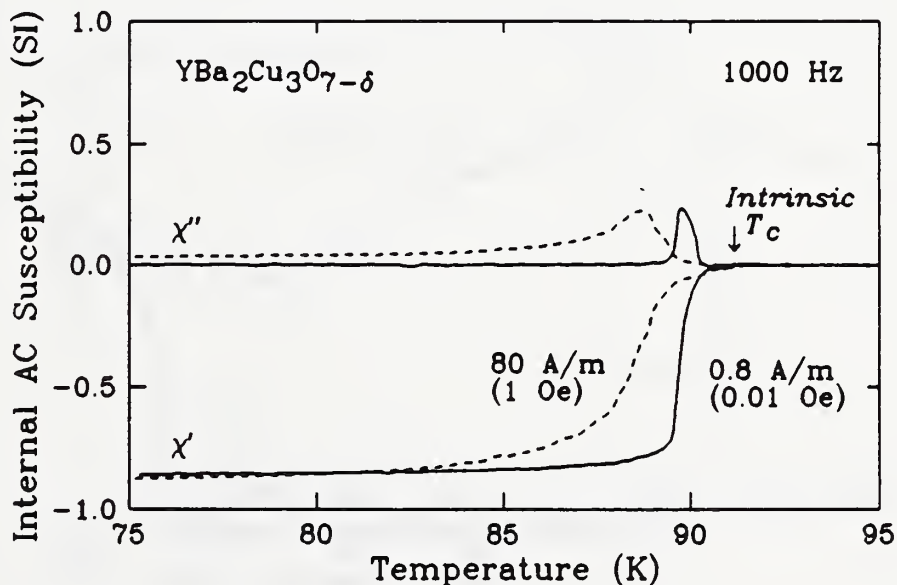


Fig. 2. Internal ac susceptibility for sintered  $\text{YBa}_2\text{Cu}_3\text{O}_{7-\delta}$  with weak coupling measured in  $0.8 \text{ A}\cdot\text{m}^{-1}$  and  $80 \text{ A}\cdot\text{m}^{-1}$  rms at  $1000 \text{ Hz}$ . Even for the lower measurement field, the coupling  $T_c$  ( $90.3 \text{ K}$ ) is measurably below the intrinsic  $T_c$  ( $91.1 \text{ K}$ ). The sample was approximately a cylinder, diameter  $0.9 \text{ mm}$ , length  $5 \text{ mm}$ . The real part does not extrapolate to  $-1$  because the sample volume used to compute susceptibility was approximate.

The critical temperature is sometimes taken as the midpoint of the diamagnetic transition and the width of the transition is quoted.<sup>43</sup> There are several problems with this. First, there are two transitions. Second, the widths of the transitions are field dependent. Third, a large part of the transition to full diamagnetism is due to coupling. Fourth, the complete intrinsic transition is often obscured by the coupling transition. Therefore, it is more useful to define the critical temperatures as the onset temperatures, although the precise onset temperatures are uncertain, particularly due to fluctuation effects.

Figure 3 shows ac susceptibility and ac resistance measured on a bar of  $(\text{Bi-Pb})_2\text{Sr}_2\text{Ca}_2\text{Cu}_3\text{O}_x$ . To compare resistivity and susceptibility curves, we first

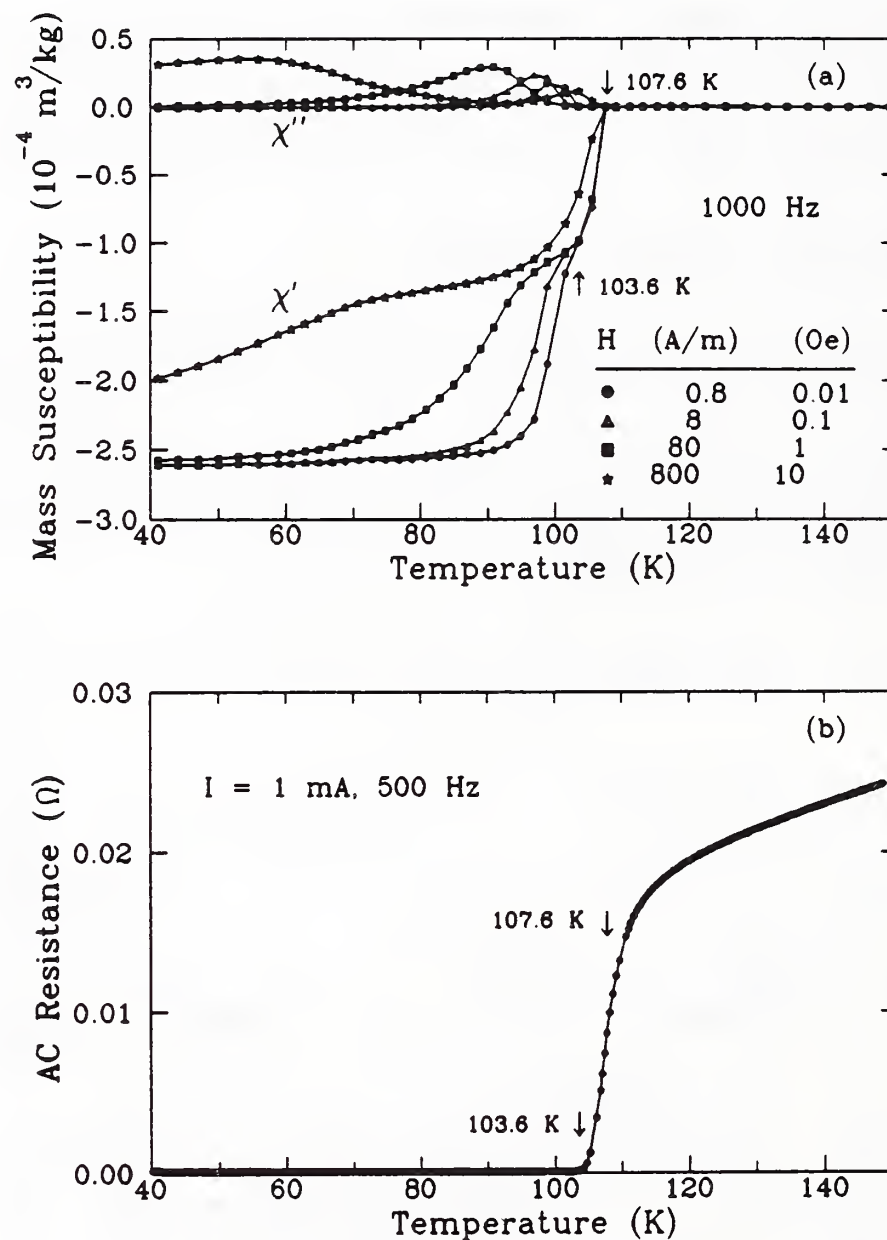


Fig. 3. Comparison of ac susceptibility and resistance as functions of temperature for  $(\text{Bi-Pb})_2\text{Sr}_2\text{Ca}_2\text{Cu}_3\text{O}_x$ . (a) Mass susceptibility for four ac fields (rms values shown) at 1000 Hz. Intrinsic  $T_c$  is 107.6 K and, for the smallest measuring field, coupling  $T_c$  is 103.6 K. (b) Resistance for an ac measuring current of 1 mA rms at 500 Hz. The critical temperatures obtained from susceptibility are labeled.

calculate the self-field of the transport current used in the resistivity measurements. For a sample with circular cross section and uniform current density, the field inside the sample is  $H(r) = rI/(2\pi a^2)$ , from Ampère's circuital law, where  $r$  is the radial coordinate,  $I$  is the current, and  $a$  is the sample radius. The average field obtained by integration over the sample cross section (rather than over the radius) is  $\langle H \rangle = I/(3\pi a)$ . For our sample (actually of rectangular cross section with an effective radius  $a \approx 0.7$  mm), the self-field of the transport current (1 mA) is negligible compared to any of the measuring fields, and the best comparison is with the lowest-field susceptibility curve. Intrinsic  $T_c$  is 107.6 K and coupling  $T_c$  for the lowest-field measurement is 103.6 K, as seen in Fig. 3(a). These temperatures are identified in the plot of resistance, Fig. 3(b).

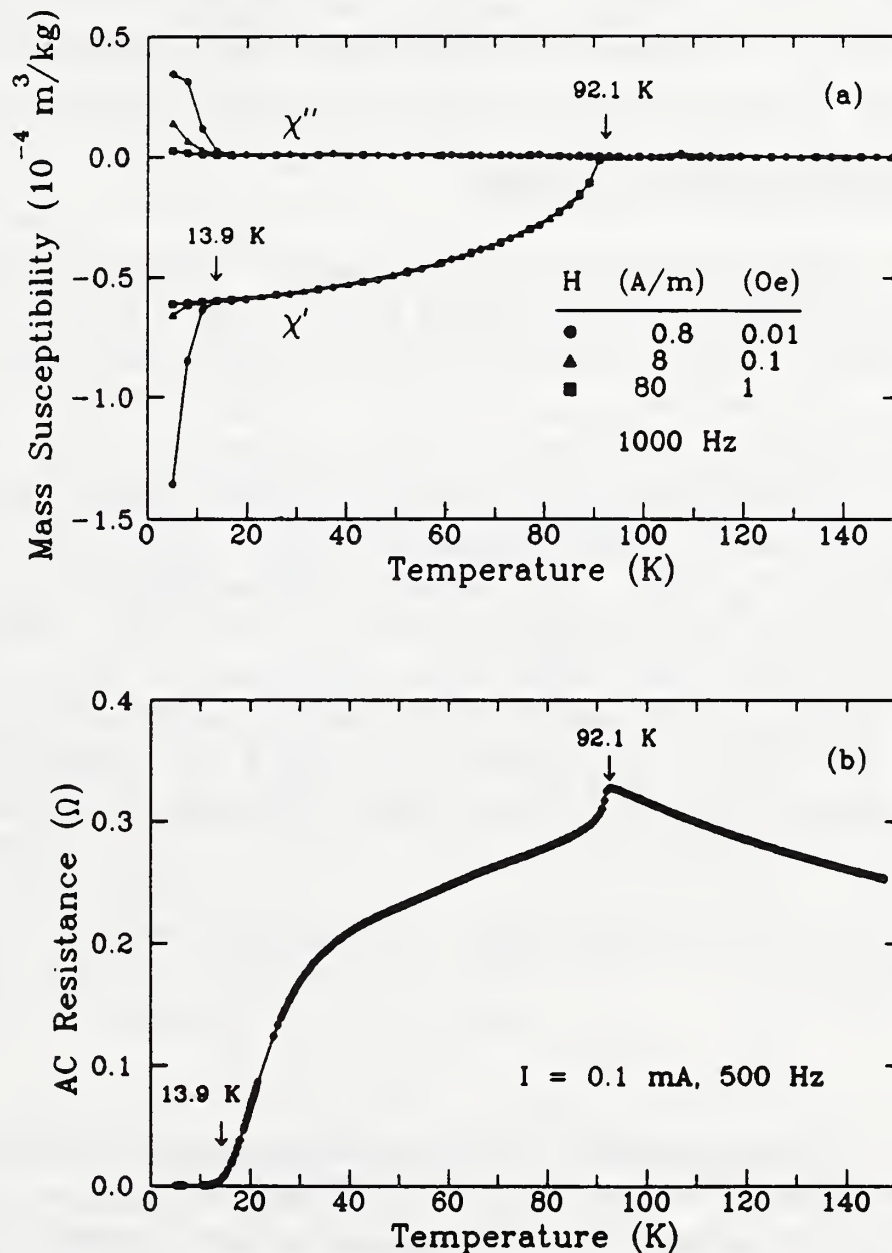


Fig. 4. Comparison of ac susceptibility and resistance as functions of temperature for YBa<sub>2</sub>Cu<sub>3</sub>O<sub>7-δ</sub> with extremely weak intergranular coupling. (a) Mass susceptibility for three ac fields (rms values shown) at 1000 Hz. Intrinsic  $T_c$  is 92.1 K and, for the smallest measuring field, coupling  $T_c$  is 13.9 K. (b) Resistance for an ac measuring current of 0.1 mA rms at 500 Hz. The critical temperatures obtained from susceptibility are labeled. The intrinsic critical temperature is unambiguous for this sample, which is semiconducting in the normal state.

The positive slope of the resistance curve above  $T_c$  indicates a normal conductor and the intrinsic  $T_c$  does not correspond to a distinguishing feature. Coupling  $T_c$  coincides with the zero-resistance temperature.

Figure 4 shows ac susceptibility and ac resistance measured on a bar of sintered Y-Ba-Cu-O with extremely weak intergranular coupling. The comparison is informative. From Fig. 4(a), intrinsic  $T_c$  is 92.1 K but coupling  $T_c$  is only 13.9 K and very field dependent. In Fig. 4(b), there is a peak in the resistance curve at the intrinsic  $T_c$  where the material goes from the semiconducting state to the superconducting state. Resistance is zero at about the coupling  $T_c$ . In summary, the temperature for zero resistivity is related to the susceptibility coupling onset temperature, which is determined by the quality of intergrain coupling. The temperature for the initial drop in resistivity is related to the intrinsic onset temperature, which is determined by the quality of the grains. Other experimental studies are consistent with these conjectures.<sup>44-49</sup>

## DEMAGNETIZING FACTORS

Demagnetizing factors are important for the understanding of the susceptibility of superconductors and especially films. In the equation for magnetic induction,  $B = \mu_0(H + M)$ ,  $H$  is the internal field, equal to the external or applied field  $H_a$  corrected by the demagnetizing field  $H_d$ . The source of the demagnetizing field is taken to be magnetic poles on the surface of a magnetized specimen. In ellipsoids, the poles are distributed in such a way that all fields are uniform. These fields include  $H_a$ ,  $H_d$ , and  $H$ , and the magnetization  $M$ . They are related vectorially by the equation  $H = H_a + H_d = H_a - \mathbf{N}M$ , where  $\mathbf{N}$  is the demagnetizing tensor. If  $H_a$  is along a principal axis of the ellipsoid, then  $H = H_a + H_d = H_a - NM$ , where  $N$  is the scalar demagnetizing factor. (If  $H_a$  is not along a principal axis of the ellipsoid and  $\chi \neq 0$ ,  $M$  is uniform but not coaxial with  $H_a$ , and the direction and magnitude of  $M$  depend on  $\chi$ .) For ellipsoids of revolution (spheroids)  $N$  is a function of the aspect ratio  $\gamma$  of the ellipsoid (ratio of the polar axis to the equatorial axis) and is independent of susceptibility  $\chi$ .<sup>50,51</sup>

$$N = (1 - \gamma^2)^{-1}[1 - \gamma(1 - \gamma^2)^{-1/2}\cos^{-1}\gamma] \quad (\gamma < 1), \quad (1a)$$

$$N = \frac{1}{3} \quad (\gamma = 1), \quad (1b)$$

$$N = (\gamma^2 - 1)^{-1}[\gamma(\gamma^2 - 1)^{-1/2}\cosh^{-1}\gamma - 1] \quad (\gamma > 1). \quad (1c)$$

Demagnetizing factors for cylinders have been examined in detail by Chen, Brug, and Goldfarb.<sup>52</sup> For cylinders,  $N$  is a function of  $\gamma$  (ratio of length to diameter) and also  $\chi$ , which is assumed to be constant in the sample. With  $H_a$  along the cylinder axis,  $M$  and  $H_d$  are both nonuniform except in two cases. When  $\chi = 0$ ,  $M$  is uniform. The approximation  $\chi = 0$  is used for saturated ferromagnets, diamagnets, and paramagnets. When  $\chi \rightarrow \infty$ ,  $H_d$  is uniform and equal to  $-H_a$ . The condition  $\chi \rightarrow \infty$  applies to soft ferromagnetic materials. When  $\chi = -1$ ,  $(M + H_d)$  is uniform and equal to  $-H_a$ . [That is,  $B = \mu_0(H_a + H_d + M) = 0$ .] This applies to superconductors in the shielding state.

There are two types of demagnetizing factors for cylinders. The fluxmetric (or ballistic) demagnetizing factor  $N_f$  is the ratio  $-\langle H_d \rangle_s / \langle M \rangle_s$ , where  $\langle \rangle_s$  indicates an

Table 1. Longitudinal and transverse magnetometric demagnetizing factors  $N_{mz}$  and  $N_{mx}$  for cylinders with  $\chi = -1$ , after Taylor.<sup>53</sup>  $\gamma$  is the ratio of length to diameter.

$\gamma$	$N_{mz}$	$N_{mx}$
0	1	0
0.25	0.6764	0.2136
0.5	0.5258	0.2928
1	0.3692	0.3669
2	0.2341	0.4237
4	0.1361	0.4596
$\infty$	0	0.5

average over the center plane of the cylinder. The magnetometric demagnetizing factor  $N_m$  is the ratio  $-\langle H_d \rangle_v / \langle M \rangle_v$ , where  $\langle \rangle_v$  indicates an average over the volume of the cylinder. Fluxmetric factors are used when magnetization is measured ballistically, with a short search coil closely wrapped around the center of a long sample. Magnetometric factors are used with magnetometers that sense the entire sample volume, such as vibrating-sample magnetometers, SQUID magnetometers, and ac susceptometers. Both  $N_f$  and  $N_m$  depend on  $\gamma$  and  $\chi$ .

Experimental and theoretical work on demagnetizing factors for cylinders dates back to the 1880s. However, perhaps the only research ever published until recently for  $\chi = -1$  was Taylor's paper on conducting cylinders.<sup>53</sup> He calculated polarizabilities, which we can convert to  $N_m$ , for several values of  $\gamma$  for both longitudinal and transverse fields. Our reduction of his results is given in Table 1.<sup>52</sup> Note that  $N_{mx} + N_{my} + N_{mz} = 2N_{mx} + N_{mz} \geq 1$ . The subscripts  $x, y, z$  indicate the orthogonal axes, with the applied field along  $z$ . (The sum of the three orthogonal magnetometric demagnetizing factors for cylinders equals 1 only when  $\chi = 0$ .)  $N_m$  and  $N_f$  for the complete range of  $\gamma$  and  $\chi$  are given in Ref. 52. Values of  $N_m$  for  $\chi = -1$  are different from those often tabulated for  $\chi = 0$ . For  $\gamma = 1$ , for example,  $N_{mz} = 0.3116$  for  $\chi = 0$ . One caveat is that values of  $N_m$  for  $\chi = -1$  are for superconductors in the shielding state. Superconductors in the mixed state do not have constant susceptibility, which is one of the basic assumptions in the derivation.

The measurement of susceptibility requires the application of  $H_a$  and the measurement of  $M$ . The susceptibility  $dM/dH_a$  is characteristic of the *sample* and may be termed the *external* susceptibility  $\chi_{ext}$ . The *internal* susceptibility  $\chi$ , characteristic of the *material*, is  $dM/dH$ . The two susceptibilities are related:  $\chi = \chi_{ext}/(1 - N\chi_{ext})$  and  $\chi_{ext} = \chi/(1 + N\chi)$ . When ac susceptibility is measured,  $\chi_{ext}$  is a complex quantity:  $\chi_{ext} \equiv \chi'_{ext} + i\chi''_{ext}$ . The internal susceptibility is also complex:  $\chi \equiv \chi' + i\chi''$ . When relating the two quantities  $\chi$  and  $\chi_{ext}$ , the real parts and the imaginary parts are separated, resulting in

$$\chi' = [\chi'_{ext} - N(\chi'_{ext}{}^2 + \chi''_{ext}{}^2)] / [N^2(\chi'_{ext}{}^2 + \chi''_{ext}{}^2) - 2N\chi'_{ext} + 1], \quad (2a)$$

$$\chi'' = \chi''_{ext} / [N^2(\chi'_{ext}{}^2 + \chi''_{ext}{}^2) - 2N\chi'_{ext} + 1]. \quad (2b)$$

This rule appears periodically in the literature.<sup>54-56</sup> (We should point out that an interesting artifact occurs in these equations for  $\chi'$  and  $\chi''$  in terms of  $\chi'_{ext}$ ,  $\chi''_{ext}$ , and  $N$ . When  $N \approx 1$  and  $\chi'_{ext} \approx 1$  and  $\chi''_{ext} \approx 0$ , as might occur for films in the normal state,  $\chi'$  and  $\chi''$  diverge, causing severe scatter in  $\chi'$  and  $\chi''$ . Such values of  $\chi'_{ext}$  and  $\chi''_{ext}$  are not uncommon in actual measurements of thick films.)

### *Volume Fraction of Superconductor Grains*

When the ideal ("X-ray") density of a superconductor is known, and when there are no nonsuperconducting phases present, the volume fraction of superconducting grains can be estimated from mass and volume measurements. Otherwise, susceptibility curves give some information on the volume fraction. When grains are fully coupled, the entire volume of a granular sample, including voids and nonsuperconducting phases, is shielded and  $\chi = -1$ . When grains are uncoupled, the inductive susceptibility signal represents a summation of shielding signals from many grains; voids and nonsuperconducting phases do not contribute.

Consider a sintered pellet of spherical superconductor grains, each with susceptibility  $\chi_g = -1$ , occupying a volume fraction  $\phi$  in a medium of  $\chi_v = 0$ . Let the measuring magnetic field strength be large enough to decouple the grains. The demagnetizing factor of each sphere is  $\frac{1}{3}$ . Let the bulk pellet have a very different demagnetizing factor (0, for example). If the total internal susceptibility  $\chi$  is based on the volume of the bulk pellet, including voids, can one deduce  $\phi$  from the value of  $\chi$  ( $|\chi| \leq 1$ )? When we first addressed this problem<sup>17</sup> we suggested that, for grains of unknown geometry,  $\phi \approx |\chi|$ .

The susceptibility of mixtures was discussed by Maxwell in his *Treatise*.<sup>57</sup> For perfectly conducting spheres in a nonmagnetic medium, the exact relationship is  $\chi = -3\phi/(2 + \phi)$ , or  $\phi = -2\chi/(3 + \chi)$ , where  $\chi$  is the internal susceptibility of the mixture. One implication is that, for dense pellets ( $\phi \rightarrow 1$ ), the effective demagnetizing factor for a susceptibility measurement is that of the *pellet*, not that of the grains, even when the grains are decoupled. (If demagnetizing fields are thought of as arising from surface magnetic poles, a dense mixture will have pole cancellation except at the surface of the pellet.) The effective susceptibility of granular superconductors, including the effect of magnetic penetration depth, has been examined recently.<sup>58-60</sup>

When the magnetic penetration depth  $\lambda$  is on the order of the grain size, a significant fraction of the grain volume does not contribute to the  $\chi$  signal.<sup>61</sup> Typically,  $\lambda$  is on the order of  $0.2 \mu\text{m}$  in high- $T_c$  superconductors below  $\frac{1}{2}T_c$ .<sup>62-68</sup> For illustration,<sup>69</sup> a 100% dense sample composed of *uncoupled* plates of thickness  $10 \mu\text{m}$  would have, for  $H$  in the plane of the plates,  $\chi = -0.7$ . The reduction in  $\chi$  is especially severe near  $T_c$ , where  $\lambda$  becomes quite large:  $\lambda(T)/\lambda(0) = [1 - (T/T_c)^n]^{-1/2}$ , where  $n = 4$  in the two-fluid model,<sup>70</sup> but empirically  $n \approx 1$  for Y-Ba-Cu-O.<sup>62</sup>

Therefore, to estimate the volume fraction of superconducting grains in a sintered sample containing voids and nonsuperconducting inclusions: (1) The grains should be decoupled by using measuring fields large enough to depress the coupling transition

temperature. Thereby, voids and nonsuperconducting phases are not included in the shielded volume. (2) The grain dimensions should be significantly greater than  $\lambda$  so that a large fraction of the grain volume is shielded. Otherwise,  $\lambda$  should be included in the estimation. (3) The  $\chi$  value used to estimate the volume fraction should be taken well below the intrinsic  $T_c$  of the grains. This avoids the increase in  $\lambda$  near  $T_c$ . Chen *et al.* have precisely modeled  $\chi(T)$  and  $\chi(H)$  curves and calculated the volume fraction of grains using  $\lambda$  and the critical-state model for both grains and matrix. They deduced the existence of grain *clusters* in some samples based on discrepancies between actual volume fractions and those computed from the susceptibility data.<sup>71,72</sup>

A destructive way to obtain the volume fraction of superconducting grains is to crush the sample pellet, collect all the powder, and use the original sample volume to compute  $\chi$ . For loosely packed powder, the appropriate demagnetizing factor would be closer to that of a grain, typically approximated as a sphere. This is most effective when the crushing simply separates the grains from each other. If the grains were finely pulverized, their size may approach  $\lambda$ .

## SUSCEPTIBILITY OF SUPERCONDUCTOR FILMS

To easily distinguish the superconducting and normal states, resistivity is best measured in specimens with at least one thin dimension. Susceptibility, in contrast, is best measured when there is a large sample volume. Susceptibility measurements on films thus present special problems and require some interpretation. In measuring the susceptibility of films there are considerations of adequate shielded volume, field orientation with respect to the film plane, demagnetizing-factor corrections, and film thickness compared to  $\lambda$ .

### *“The Absurdity of This Result ...”*

The magnetic susceptibility of superconductor films measured in perpendicular fields presents a paradox arising from perfect diamagnetism and a demagnetizing factor  $N$  that approaches 1. For perfectly shielded superconductors,  $\chi = -1$ , so  $\chi_{ext} = -(1 - N)^{-1}$ . As superconductor films get thinner,  $N \rightarrow 1$  and  $\chi_{ext} \rightarrow -\infty$ . In the early days of electromagnetism, Maxwell commented, “If the value of  $\kappa$  [susceptibility] could be negative and equal to  $1/(4\pi)$  [in CGS units, 1 in SI units] we should have an infinite value of the magnetization in the case of a magnetizing force acting normally to a flat plate or disk. The absurdity of this result confirms what we said in Art. 428.”<sup>73</sup>

Magnetization  $M$  is the measured magnetic moment  $m$  per sample volume  $V_s$ . As the superconductor gets thinner (with its cross sectional area constant),  $\chi_{ext} \rightarrow -\infty$  because  $V_s \rightarrow 0$ , not because  $m \rightarrow -\infty$ .<sup>74</sup> Furthermore, as the film gets *very* thin and  $N \approx 1$ , flux immediately penetrates the film for any  $H_a$  and the superconductor is no longer in the shielding state.<sup>75</sup> But is not  $m$  linearly proportional to  $V_s$  or thickness  $t$ ? If it were,  $M$  would be independent of  $t$ . We will show that, for a range of  $t$ ,  $m$  remains constant for thick films of constant diameter  $d$ . Since a susceptometer pick-up coil voltage  $v$  is proportional  $m$ , this means that  $v$  is independent of  $t$ . The reason for this singular behavior is that, as  $t \rightarrow 0$ ,  $(1 - N)$  becomes proportional to  $t$ .

We model a circular superconductor film as an oblate ellipsoid, with major axes equal to the diameter  $d$  and minor axis equal to  $t$ . The ellipsoid volume  $V_s = \frac{1}{6}\pi\gamma d^3$ , where  $\gamma$  is the aspect ratio  $t/d$ . For small  $\gamma$ ,<sup>50,51</sup>  $N = 1 - \frac{1}{2}\pi\gamma + 2\gamma^2$ . For  $\gamma \leq 0.003$ , the first two terms alone give  $N$  accurate to four significant figures. We use the linear approximation and  $\chi_{ext} = m/(V_s H_a) = -(1 - N)^{-1}$  to get:  $m = -V_s H_a/(1 - N) = -\frac{1}{3}d^3 H_a$  (independent of  $t$ )<sup>76,77</sup> and a gauge for superconductor films,

$$\chi_{ext} = -2/(\pi\gamma). \quad (3)$$

For computational convenience, we extrapolate these arguments to a flat cylinder:  $V_s = \frac{1}{4}\pi\gamma d^3$  and  $m = -\frac{1}{2}d^3 H_a$ .

The magnetic moment of a superconductor arises from shielding currents which, for small applied fields, flow within a penetration depth  $\lambda$  of the surface. If we consider a cylinder of diameter  $d$  and height  $t$ , the magnetic moment of the current loop is  $m = -\frac{1}{4}\pi d^2 I$ , where  $I$  is the total shielding current. In terms of a current density  $J$ ,  $m = -\frac{1}{4}\pi d^2 J \lambda t$ , which is equal to a constant from the previous discussion. (Strictly, the shielding current in a superconducting cylinder does not flow in a uniformly wide sheath on its circumference.) What happens when  $t$  gets too small? As  $t$  decreases  $J$  must increase until it equals the critical current density  $J_c$ . Any further decrease in  $t$  will result in flux penetration into the superconductor. From  $m = -\frac{1}{2}d^3 H_a = -\frac{1}{4}\pi d^2 J \lambda t$ , the critical thickness  $t_c$  is simply  $2H_a d/(\pi J_c)$ , which offers a way to determine  $J_c$  if  $\lambda$  is known. The analysis breaks down for thin films ( $t \rightarrow \lambda$ ) for which there is an enhanced effective  $\lambda$ .<sup>78</sup>

We have experimentally verified some of these points with a series of seven superconducting Bi-Sr-Ca-Cu-O thick films. They were made by metallo-organic decomposition and had the usual granular characteristics. Their diameter was 3.22 mm and they ranged in thickness from 2.8 ( $\pm 0.2$ )  $\mu\text{m}$  to 0.37 ( $\pm 0.02$ )  $\mu\text{m}$ . Plots of  $\chi'_{ext}$  as a function of temperature, measured in a field of 0.8 A  $\cdot$  m<sup>-1</sup>, 1000 Hz, normal to their surface, were almost flat at low temperatures and indicated good diamagnetic shielding at 4.2 K for all except the 0.37- $\mu\text{m}$  film.  $\chi'_{ext}$  at 4.2 K ranged from -390 for the 2.8- $\mu\text{m}$  film to -2080 for the 0.55- $\mu\text{m}$  film. ( $\chi'_{ext}$  was -2560 for the 0.37- $\mu\text{m}$  film.) These values are about half those expected from  $\chi_{ext} = -2/(\pi\gamma)$ , which is not unreasonable considering the approximations involved. The pick-up coil voltages that gave rise to these  $\chi'_{ext}$  ranged from 4.0 to 4.4  $\mu\text{V}$  (almost constant). The 0.37- $\mu\text{m}$  film voltage was smaller, 3.6  $\mu\text{V}$ . The imperfect shielding for the 0.37- $\mu\text{m}$  film suggests that  $t_c \approx 0.4 \mu\text{m}$ .

### ***Dependence on Field Angle***

When the field is perpendicular to the superconductor film plane there is more susceptometer signal than when the field is parallel. Aside from considerations regarding magnetic penetration depth, the reason is that, for the perpendicular orientation ( $N \approx 1$ ), the applied field  $H_a$  is enhanced to give a large internal field,  $H = H_a/(1 - N)$ , and so are the magnetization,  $M = -H_a/(1 - N)$ , and the external susceptibility,  $\chi_{ext} = -(1 - N)^{-1}$ . (For magnetically soft, ferromagnetic films, in comparison,  $\chi \rightarrow \infty$  and  $\chi_{ext} \rightarrow N^{-1}$ .)

Misalignment of a superconductor film in a magnetometer or susceptometer causes errors in the measurement of  $\chi_{ext}$ . For example, Gyorgy found that  $\chi_{ext}$  of a Nb film of dimensions  $7.6 \text{ mm} \times 5 \text{ mm} \times 0.13 \text{ } \mu\text{m}$  varied from  $-0.08$ , for  $H_a$  parallel to the film surface, to  $-0.17$  for  $H_a$  at an angle of  $0.5^\circ$  from the film plane, to  $-18$  for  $H_a$  at an angle of  $8^\circ$ .<sup>79</sup> Teshima *et al.* studied the angular dependence of the mixed-state magnetic hysteresis loop and concluded that the magnetization is perpendicular to the film plane for any direction of the applied field.<sup>80</sup>

We can examine the field-angle problem analytically. We start by modeling the film as an isotropic (constant  $\chi$ ), oblate ellipsoid. We use the relations

$$H_{a,\zeta} = H_\zeta + N_\zeta M_\zeta = H_\zeta(1 + N_\zeta \chi), \quad (4a)$$

$$M_\zeta = \chi H_\zeta = \chi H_{a,\zeta} / (1 + N_\zeta \chi) = H_{a,\zeta} / (\chi^{-1} + N_\zeta), \quad (4b)$$

where the subscript  $\zeta$  denotes the three ellipsoid axes  $x, y, z$ .  $H_a$  is at an angle  $\theta$  with respect to the normal to the film plane ( $z$  axis), so  $H_{a,z} = H_a \cos\theta$  and  $H_{a,x} = H_a \sin\theta$ . For a superconductor in the shielding state, we take  $\chi = -1$ . Using  $2N_x + N_z = 1$ , we have

$$M_z = -H_a \cos\theta / (1 - N_z), \quad (5a)$$

$$M_x = -H_a \sin\theta / (1 - N_x) = -2H_a \sin\theta / (1 + N_z). \quad (5b)$$

But we measure  $M$  only in the axis of  $H_a$ , that is,  $M_z \cos\theta + M_x \sin\theta$ , so our measured susceptibility is

$$\chi_{ext} = -\cos^2\theta / (1 - N_z) - 2\sin^2\theta / (1 + N_z). \quad (6)$$

For superconductor films ( $N_z \rightarrow 1$ ), a slightly out-of-plane  $H_a$  ( $\theta < \frac{1}{2}\pi$ ) will cause  $M_z$  to dominate. The same analysis for magnetically soft, ferromagnetic ellipsoids ( $\chi \rightarrow \infty$ ) gives

$$M_z = H_a \cos\theta / N_z, \quad (7a)$$

$$M_x = 2H_a \sin\theta / (1 - N_z), \quad (7b)$$

$$\chi_{ext} = \cos^2\theta / N_z + 2\sin^2\theta / (1 - N_z). \quad (8)$$

For ferromagnetic films, a slightly off-axis  $H_a$  ( $\theta > 0$ ) will cause much of the magnetization to be in plane.

### **Multiple Phases**

When susceptibility is measured as a function of temperature in perpendicular field,  $\chi_{ext}$  curves appear strikingly different from the  $\chi$  curves obtained after correcting for demagnetizing factor. Measurements made with the field perpendicular to the film plane give very large values of external susceptibility. Values of  $-1500$  for  $\chi'_{ext}$  are typical. However, when corrected for demagnetizing factor, any large negative value of  $\chi'_{ext}$  will convert to  $\chi' \approx -1$ ; there is negligible difference in  $\chi'$  between  $\chi'_{ext} = -1500$

and  $\chi'_{ext} = -15$ . Furthermore, huge errors in volume will barely affect the  $\chi'$  result. The obvious way to avoid these difficulties is to measure  $\chi$  with the field parallel to the plane of the film. However, this arrangement gives inadequate signal if the sample volume is insufficient or if the magnetic penetration depth is large relative to the film thickness. Furthermore, it is sometimes difficult to align films perfectly parallel to the applied field. If these problems arise, one has to resort to measurements in perpendicular field in which  $\chi_{ext}$  is measured and  $\chi$  is computed.

Superconducting Bi–Sr–Ca–Cu–O thick films, about 1  $\mu\text{m}$  thick, were prepared by metallo-organic decomposition on single-crystal (100)-oriented MgO substrates.<sup>81–83</sup> By adjusting the heat treatment of the films, we varied the relative concentration of the two superconducting phases,  $\text{Bi}_2\text{SrCa}_2\text{Cu}_2\text{O}_x$  (“2122,” nominal  $T_c = 85$  K) and  $\text{Bi}_2\text{Sr}_2\text{Ca}_2\text{Cu}_3\text{O}_x$  (“2223,” nominal  $T_c = 110$  K). Each phase had both intrinsic and coupling components. The films were highly oriented, composed of platelets with  $c$  axes perpendicular to the film plane. The platelets were 10–30  $\mu\text{m}$  wide and 0.2–0.3  $\mu\text{m}$  thick. The films were characterized by X-ray diffraction, electrical resistivity, and ac susceptibility in parallel and perpendicular fields with the intent of ascertaining the relative concentration of the 2212 and 2223 phases.

The areas of the low-angle (002) X-ray diffraction peaks give a relative measure of the concentration of the two phases.<sup>84</sup> (Diffraction does not distinguish between intrinsic and coupling components.) For the (002) reflection, 50% of the signal comes from the top 0.16  $\mu\text{m}$  of the film. This is important because phase segregation through the film thickness is likely. Resistivity provides evidence of two phases, but the lower-temperature 2212 phase will not be detected once the concentration of the higher-temperature 2223 phase exceeds the percolation threshold. Thus, the relative magnitudes of the resistivity transitions will give only a hint of the phase fractions.

For susceptibility, which is more useful,  $\chi_{ext}$  or  $\chi'$ ? As noted above, the demagnetization correction to obtain  $\chi'$  from  $\chi'_{ext}$  is nonlinear. Thus  $\chi'_{ext}$  gives a better indication of the relative fractions of the different intrinsic phases. The coupling components should not be included in the determination; this might require measurements at several fields. (As expected, we found that the coupling component was tied to the “parent” phase. In single-phase 2212 samples, for example, there was no 2223 coupling component.)  $\chi$ , highly nonlinear, is useful for highlighting the transition temperature of each phase, especially the higher-temperature 2223 phase, which is often obscured in  $\chi_{ext}$ . One strategy for determining the phase fractions, not suitable for routine measurements, is to scrape the films into a powder and measure its susceptibility, thus eliminating the coupling components and reducing the demagnetizing factor problem. Perhaps the major utility of susceptibility measurements in granular superconductors, however, is for characterizing the quality of intergrain coupling by the field dependence of the coupling transition temperature.

In Table 2 we give values of the percentages of the 2212 and 2223 phases as inferred from resistivity, X-ray diffraction, and susceptibility, for one of the films while intact and after powdering. The presence of a small amount of  $\text{Bi}_2\text{Sr}_2\text{CuO}_6$  was ignored except in the X-ray determinations, which do not sum to 100. As far as we

Table 2. Volume percentage of 2212 and 2223 phases in a Bi–Sr–Ca–Cu–O film as inferred from different measurement methods.

Morphology	Method	2212	2223
Film	$\rho$	5	95
Film	X-ray	12	82
Film	$\chi'_{ext}$ , $H \parallel$	75	25
Film	$\chi'_{ext}$ , $H \perp$	60	40
Powder	X-ray	32	47
Powder	$\chi'_{ext}$	30	70
Powder	$\chi'$	40	60

know, none of these determinations is “correct.” Our intent is to illustrate the difficulty of the problem.

## UNITS

Magnetic volume susceptibility  $\chi$  is  $dM/dH$  in both SI and CGS. In terms of base units,  $\chi$  is a dimensionless quantity. In CGS, however,  $\chi$  is usually expressed as emu,  $\text{emu}\cdot\text{cm}^{-3}$ , or  $\text{emu}\cdot\text{cm}^{-3}\cdot\text{Oe}^{-1}$ . The designation “emu” is merely an indicator that electromagnetic units are in use; it is not a unit. The unusual  $\chi$  units in CGS arise from ambiguity in the units for  $M$ .<sup>85</sup> In CGS,  $H$  is in Oe (dimensionally and numerically equivalent to G). Magnetization, when written as  $4\pi M$ , is in G. When magnetization is expressed simply as  $M$  (the magnetic moment  $m$  per unit volume) its units are  $\text{erg}\cdot\text{G}^{-1}\cdot\text{cm}^{-3}$  (conventionally expressed as  $\text{emu}\cdot\text{cm}^{-3}$ ), which are dimensionally but *not numerically* equivalent to G. Occasionally, CGS susceptibility is written as  $4\pi\chi$  (dimensionless), which is equal to SI susceptibility (dimensionless).

Some of the symbols used in this paper and their associated SI units are  $M$  [ $\text{A}\cdot\text{m}^{-1}$ ],  $J$  [ $\text{A}\cdot\text{m}^{-2}$ ],  $a$  [m],  $H$  [ $\text{A}\cdot\text{m}^{-1}$ ], and  $W$  [ $\text{J}\cdot\text{m}^{-3}$ ]. To convert equations to CGS EMU, replace symbols for  $H$  by  $(4\pi\mu_0)^{-1/2}H$ , symbols for  $J$  by  $(4\pi/\mu_0)^{1/2}J$ , symbols for  $M$  by  $(4\pi/\mu_0)^{1/2}M$ , symbols for  $\chi$  by  $4\pi\chi$ , and simplify as necessary. The symbols and their associated CGS EMU are  $M$  [ $\text{emu}\cdot\text{cm}^{-3}$ ],  $J$  [ $\text{abamp}\cdot\text{cm}^{-2}$ ],  $a$  [cm],  $H$  [Oe], and  $W$  [ $\text{erg}\cdot\text{cm}^{-3}$ ]. (Note that in CGS Gaussian units,  $J$  would be in  $\text{statamp}\cdot\text{cm}^{-2}$ .) We avoid the use of “practical” or mixed units.

## SUSCEPTIBILITY OF BULK SUPERCONDUCTORS, CRITICAL–STATE MODEL

In this section we review magnetic formulas for isotropic superconductors of several geometries in the Bean critical-state model.<sup>86–88</sup> Except for some of the high field susceptibility equations, most can be found in the literature in one form or another. Transport current, dc bias field, lower critical field, and surface barrier are all taken to be zero.  $H_a$  is the applied dc field.  $H_p$  is the full-penetration field, a function of the critical current density  $J_c$  (considered isotropic) and the cylinder radius (or slab half-thickness)  $a$ .  $M$  is the magnetization per unit volume of superconductor, which is equal to the half-width of the hysteresis loop ( $\frac{1}{2}\Delta M$ ) for  $H_a \geq H_p$ .  $H_m$  is the maximum

field for the hysteresis cycle, that is, the amplitude of the ac field.  $W$  is the hysteresis loss per unit volume per field cycle.  $\chi'$  and  $\chi''$  are the real and imaginary parts of ac susceptibility. The equations for  $\chi'$  and  $\chi''$  are derived from Fourier integrals of the magnetization<sup>89</sup> using the complete equations for magnetization as a function of field,<sup>90</sup> not the initial curve. By  $\chi'$  and  $\chi''$  we mean the fundamental Fourier components  $\chi'_1$  and  $\chi''_1$ . As a check, we know from first principles<sup>91,92</sup> that  $\chi'' = W/(\pi\mu_0 H_m^2)$  for any  $H_m$ . For  $H_m \gg H_p$ , the Bean hysteresis loop is almost rectangular, and  $W \rightarrow 4\mu_0 H_m M$ . A point worth emphasizing is that  $\chi' \neq \bar{\chi}_{dc} \equiv M/H_a$ . Only in the linear limit  $H_m \ll H_p$  does  $\chi' \rightarrow \bar{\chi}_{dc}$ . Another point, applicable to the cylinder in transverse field, is that the susceptibilities are based on the applied field, and are not corrected for demagnetization.

### ***Infinite Slab, Thickness $2a$ , Parallel $H$* <sup>93,94</sup>**

The equations below are for the initial magnetization curve ( $0 \leq H_a \leq H_p$ ) and the *descending* portion of the hysteresis loop (which depends on whether  $H_m \leq H_p$  or  $H_m \geq H_p$ ). To get the *ascending* portion, replace  $M$  by  $-M$  and  $H_a$  by  $-H_a$  in the equations. For example, the ascending magnetization curve for  $H_m \leq H_p$  is  $M = -H_a - \frac{1}{4}(H_m^2 - 2H_a H_m - H_a^2)/H_p$ , based on Eq. (11). To calculate  $\chi'$  and  $\chi''$  we use  $H_a = H_m \cos\theta$ . For  $H_m \geq H_p$ , we integrate from  $\theta = 0$  to  $\cos^{-1}(1 - 2/x)$ , and from  $\theta = \cos^{-1}(1 - 2/x)$  to  $\pi$ , where  $x \equiv H_m/H_p$ . A useful trigonometric identity is  $\sin[\cos^{-1}(1 - 2/x)] = (2/x)(x - 1)^{1/2}$ .

$$H_p = J_c a \quad (9)$$

$$M = -H_a + \frac{1}{2}H_a^2/H_p \quad (0 \leq H_a \leq H_p) \quad (10)$$

$$H_m \leq H_p: M = -H_a + \frac{1}{4}(H_m^2 + 2H_a H_m - H_a^2)/H_p \quad (-H_m \leq H_a \leq H_m) \quad (11)$$

$$W = \frac{2}{3}\mu_0 H_m^3/H_p \quad (12)$$

$$\chi' = -1 + \frac{1}{2}x \quad (13)$$

$$\chi'' = 2x/(3\pi) \quad (14)$$

$$H_m \geq H_p: M = -\frac{1}{2}H_p + H_m - H_a - \frac{1}{4}(H_m - H_a)^2/H_p \quad (H_m - 2H_p \leq H_a \leq H_m) \quad (15a)$$

$$M = \frac{1}{2}H_p \quad (-H_m \leq H_a \leq H_m - 2H_p) \quad (15b)$$

$$W = 2\mu_0 H_m H_p - \frac{4}{3}\mu_0 H_p^2 \quad (16)$$

$$\chi' = \{(-1 + \frac{1}{2}x) \cos^{-1}(1 - 2/x) + [-1 + 4/(3x) - 4/(3x^2)](x - 1)^{1/2}\} / \pi \quad (17)$$

$$\chi'' = (6/x - 4/x^2)/(3\pi) \quad (18)$$

### ***Infinite Cylinder, Radius $a$ , Axial $H$* <sup>93,95-98</sup>**

$$H_p = J_c a \quad (19)$$

$$M = -H_a + H_a^2/H_p - \frac{1}{3}H_a^3/H_p^2 \quad (0 \leq H_a \leq H_p) \quad (20)$$

$$H_m \leq H_p: M = -H_a + \frac{1}{2}(H_m^2 + 2H_aH_m - H_a^2)/H_p - \frac{1}{4}(H_m^3 + H_m^2H_a - H_mH_a^2 + \frac{1}{3}H_a^3)/H_p^2 \quad (-H_m \leq H_a \leq H_m) \quad (21)$$

$$W = \frac{4}{3}\mu_0H_m^3/H_p - \frac{2}{3}\mu_0H_m^4/H_p^2 \quad (22)$$

$$\chi' = -1 + x - 5x^2/16 \quad (23)$$

$$\chi'' = (4x - 2x^2)/(3\pi) \quad (24)$$

$$H_m \geq H_p: M = -\frac{1}{3}H_p + H_m - H_a - \frac{1}{2}(H_m - H_a)^2/H_p + (H_m - H_a)^3/(12H_p^2) \quad (H_m - 2H_p \leq H_a \leq H_m) \quad (25a)$$

$$M = \frac{1}{3}H_p \quad (-H_m \leq H_a \leq H_m - 2H_p) \quad (25b)$$

$$W = \frac{4}{3}\mu_0H_mH_p - \frac{2}{3}\mu_0H_p^2 \quad (26)$$

$$\chi' = \{(-1 + x - 5x^2/16) \cos^{-1}(1 - 2/x) + [-19/12 + \frac{5}{8}x + 1/x - 2/(3x^2)](x - 1)^{1/2}\} / \pi \quad (27)$$

$$\chi'' = (4/x - 2/x^2)/(3\pi) \quad (28)$$

### Infinite Cylinder, Radius $a$ , Transverse $H$

This case has not been solved exactly, but a few approaches have been used successfully. The method of Carr *et al.* gives analytic equations in the limits of small and large fields<sup>99-102</sup> and is mostly numerical in between.<sup>103</sup> The hysteresis loss in SI units is  $W = 256\mu_0H_m^3/(9\pi^2H_p)$  for  $H_m \ll H_p$ , and  $W = \frac{8}{3}\mu_0H_mH_p$  for  $H_m \gg H_p$ . The method of Zenkevitch *et al.*, presented below, gives reasonable equations for the full field range.<sup>104-106</sup> For  $M$  we preserved the form of the equations developed in Ref. 104. In terms of  $H_p$ , the equations are simply twice those for the cylinder in axial  $H$ . Different functional forms are given by other authors.<sup>107,108</sup>

$$H_p = 2J_c a / \pi \quad (29)$$

$$M = -\frac{2}{3}H_p[1 + (H_a - H_p)^3/H_p^3] \quad (0 \leq H_a \leq H_p) \quad (30)$$

$$H_m \leq H_p: M = \frac{4}{3}H_p[1 + (H_m - H_a - 2H_p)^3/(2H_p)^3] - \frac{2}{3}H_p[1 + (H_m - H_p)^3/H_p^3] \quad (-H_m \leq H_a \leq H_m) \quad (31)$$

$$W = \frac{8}{3}\mu_0H_m^3/H_p - \frac{4}{3}\mu_0H_m^4/H_p^2 \quad (32)$$

$$\chi'_{ext} = -2 + 2x - \frac{5}{8}x^2 \quad (33)$$

$$\chi''_{ext} = (8x - 4x^2)/(3\pi) \quad (34)$$

$$H_m \geq H_p: M = \frac{4}{3}H_p[1 + (H_m - H_a - 2H_p)^3/(2H_p)^3] - \frac{2}{3}H_p \quad (H_m - 2H_p \leq H_a \leq H_m) \quad (35a)$$

$$M = \frac{2}{3}H_p \quad (-H_m \leq H_a \leq H_m - 2H_p) \quad (35b)$$

$$W = \frac{8}{3}\mu_0H_mH_p - \frac{4}{3}\mu_0H_p^2 \quad (36)$$

$$\chi'_{ext} = \{(-2 + 2x - \frac{5}{8}x^2) \cos^{-1}(1 - 2/x) + [-19/6 + \frac{5}{4}x + 2/x - 4/(3x^2)](x - 1)^{1/2}\} / \pi \quad (37)$$

$$\chi''_{ext} = (8/x - 4/x^2)/(3\pi) \quad (38)$$

In Fig. 5 we plot  $\chi'$  and  $\chi''$  as functions of  $H_p/H_m$  for the three cases. As we discuss in Ref. 89,  $H_p$  is a good proxy for temperature, and the inverted abscissa in Fig. 5 is meant to indicate the temperature dependence of susceptibility. Note that, for the transverse-field case,  $\chi'_{ext} \rightarrow -2$  as  $x \rightarrow 0$ . For this geometry the demagnetizing factor is  $\frac{1}{2}$ ; after correcting for demagnetization,  $\chi' \rightarrow -1$ .

### Critical Current Density

Transport  $J_c$  is measured directly using electrical techniques.<sup>109</sup> Alternatively, several magnetic methods may be used.<sup>110</sup> To estimate  $J_c$  from magnetic measurements, one could measure  $M$  (at  $H_a \geq H_p$ ) and derive what has become known as “magnetization  $J_c$ .” Alternatively, one could measure the reduction in field  $\Delta H_a = 2H_p$  required to reverse the magnetization in the hysteresis loop.<sup>111,112</sup> Other magnetic methods are based on ac susceptibility,<sup>55,113–116</sup> usually with a dc bias field,<sup>116–119</sup> sometimes using harmonic analysis.<sup>89,93,120–122</sup> Curve fitting is often involved. For example, at the peak of  $\chi''$ ,  $H_m = H_p$  for cylinders<sup>113</sup> and  $H_m = \frac{4}{3}H_p$  for slabs<sup>108</sup> (Fig. 5). The dimensions of the sample are used in all these methods.

The equations that relate  $J_c$  to the magnetization are based on the assumption that  $J_c$  is a constant, *independent* of  $H_a$ . Apparently begging the question, the equations are often used to deduce  $J_c$  as a *function* of  $H_a$ . This is not necessarily a serious error provided that certain conditions are satisfied: (1) The sample is homogeneous and isotropic, although the critical-state model has been extended for anisotropic critical current densities.<sup>123,124</sup> (2) The sample has dimensions consistent with the model. However, in the fully penetrated state ( $H \geq H_p$ ) in the Bean formalism, the magnetization is saturated even for finite dimensions. Thus, for example, the infinite cylinder equation for  $M$  can be used for a finite disk in perpendicular field.<sup>80</sup> (3) The field at which magnetization  $M$  is taken should be large enough ( $H > H_p$ ) such that  $J_c$  is not a strong function of  $H_a$ .<sup>90</sup> Specifically, estimates of  $J_c$  from  $M$  at  $H_a = 0$  are

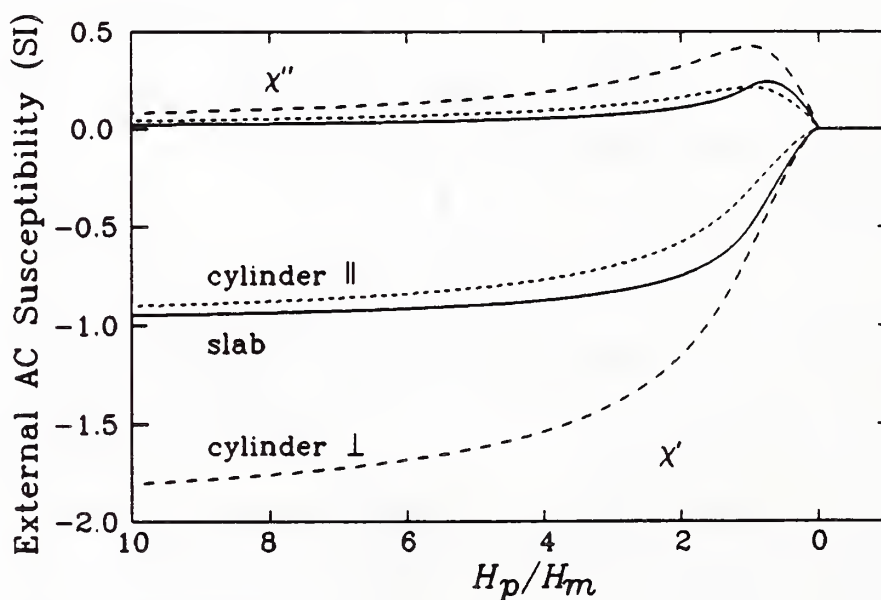


Fig. 5. External ac susceptibility for slab and cylinder geometries as functions of decreasing  $H_p/H_m \equiv x^{-1}$  based on the critical-state model.

likely to be in error. (4) Flux vortices are well pinned; that is, there is no flux creep.<sup>88</sup> In practical type-II superconductors with high  $J_c$ , or in high- $T_c$  superconductors at low temperature, this is generally true. (5) There is little contribution from surface barriers<sup>125-127</sup> and reversible magnetization.<sup>127</sup> This often applies at low temperatures, where the hysteresis loop symmetrically spans positive and negative  $M$  at high fields.

All these conditions for use of the critical-state model are seldom satisfied simultaneously. Furthermore, interpretation of the magnetization loop and application of the critical-state formulas are different for weakly linked and homogeneous samples. For weakly linked samples, such as sintered, high- $T_c$  superconductors, the magnetization at high fields gives the intragrain critical current.<sup>35</sup> The average dimension of the grains should be used to deduce  $J_c$ . In low fields the grains are coupled. The correct dimension is that of the specimen and the deduced  $J_c$  is comparable to transport  $J_c$ . But as noted above, the critical-state model cannot be used accurately at low fields, and in any event, the coupled material is not homogeneous. For homogeneous samples, such as single crystals and samples with contiguous oriented grains, the basic critical-state model can be used if the field is applied such that shielding currents flow isotropically.

### ***Lower Critical Field***

In materials with intrinsic and coupling components, there will be two lower critical fields. Generally,  $H_{c1}$  for type-II superconductors corresponds to the field at which the initial magnetization-versus-field curve deviates from linearity. In practice, detection of this field value is difficult because the deviation may be subtle, especially if the critical current density is large. However, if the magnetic field is cycled, an area, indicative of hysteresis loss, will be traced out in the  $M-H$  plane when  $H > H_{c1}$ .<sup>128-130</sup> This is effectively the field cycle used in ac susceptibility measurements, and hysteresis loss will appear as a positive imaginary part of susceptibility  $\chi''$ .<sup>98,131</sup> Therefore, when the field amplitude used in a  $\chi$  measurement exceeds  $H_{c1}$ , positive  $\chi''$  is expected and measurements of  $\chi''(T)$  at constant  $H$ ,<sup>17,132</sup> or  $\chi''(H)$  at constant  $T$ ,<sup>133</sup> may be used to deduce an upper limit for  $H_{c1}(T)$ . Equivalent to the  $\chi''(T)$  method, the corresponding feature in  $\chi'(T)$  or  $M(T)$  is a departure from full diamagnetism.<sup>129,134-136</sup>

Susceptibility and its harmonics, measured as functions of  $H$ , reveal a distinct feature at  $H_{c1}$ .<sup>122,128</sup> In another method,  $H_{c1}$  is included in an expanded critical-state model and is a function of the remanent (trapped) magnetization.<sup>137</sup> In small specimens, such as thin films, one should be aware of the enhancement in  $H_{c1}$  that arises when the magnetic penetration depth is on the order of one of the sample dimensions.<sup>27,61,69,138,139</sup>

### ***Interpretation of Peak in $\chi''$***

The critical-state model can account for many of the features in the temperature-dependent  $\chi''$  (and  $\chi'$ ) without invoking any kind of loss mechanism or irreversibility other than magnetic hysteresis. The model may even be used to describe the behavior

of the intergranular coupling component of sintered superconductors.<sup>89,140</sup> The following interpretation of the peaks in  $\chi''$  versus increasing  $T$  is based on the critical-state approach and can be applied to both the intrinsic and coupling components.<sup>17,113,119</sup> Susceptibility is measured in an ac field of constant magnitude. We divide the temperature scale into three ranges. (1) For  $T \ll T_c$ , the ac field causes shielding currents to flow on the surface of the sample and a line to be traced out in the  $M-H$  plane. There is no hysteresis because  $J < J_c$ ,  $H < H_{c1}$ , and  $\chi'' = 0$ . (2) For  $T$  somewhat below  $T_c$ ,  $J_c$  and  $H_{c1}$  have decreased and shielding currents have to flow within the sample. The hysteresis loop in the  $M-H$  plane has an area associated with it, and  $\chi'' > 0$ . The losses and  $\chi''$  attain their maximum values after supercurrents and penetrated flux reach the center of the specimen. (3) As  $T$  approaches  $T_c$ ,  $J_c$  approaches 0, and the  $M-H$  loop has collapsed. Even though  $H_{c1}$  also approaches 0, there is no area to the loop and no hysteresis loss;  $\chi'' = 0$ . This interpretation is in accordance with the expectations of the critical-state model, in which all energy losses are hysteretic and frequency independent.

Other loss mechanisms besides hysteresis may contribute to  $\chi''$  in superconductors. These losses may be classified as time-dependent or time-independent.<sup>141</sup> In particular, frequency effects may be explained by flux creep and flux flow.<sup>142-144</sup> Other frequency-dependent contributions to  $\chi''$  could be eddy currents of normal-state electrons in a two-fluid model<sup>4,145-147</sup> and vortex lattice viscosity and viscous damping.<sup>4,148-150</sup> One physical interpretation of the ac susceptibility of superconductors is in terms of BCS theory, the generation of supercurrents, and the establishment of the Meissner state.<sup>151,152</sup> Others have used a superconductor glass model and scaling with critical exponents.<sup>153,154</sup> The *time- and field-dependent* onset of irreversibility (an "irreversibility plane"), which may occur below the temperature of the  $\chi''$  onset, may be observed by the generation of odd harmonics of susceptibility.<sup>89,122</sup>

Occasionally the intrinsic  $\chi''$  peak is not apparent.<sup>155</sup> There are several cases where this is likely, with regard to granular high- $T_c$  superconductors. (1) In well coupled materials, a small measuring field will cause the coupling peak to obscure the intrinsic peak. (2) There may be insufficient total grain volume. (3) Grain sizes may be on the order of  $\lambda$ .<sup>113</sup> (4) The grains may be superconducting only on their surface; the interior is normal, perhaps owing to deficient oxygenation, or superconducting only at a lower temperature. In this state, there would be insufficient superconducting volume and therefore a low level of losses. (5) In good quality grains,<sup>145</sup>  $H_{c1}$  may be large just below  $T_c$ . If  $H_{c1}$  only falls below  $H_a$  at  $T_c$ , no  $\chi''$  peak will be seen. That is, at the temperature that flux penetrates the grain, there is no longer any bulk pinning. A larger  $H_a$  will often elicit a measurable  $\chi''$ .

### ***Upper Critical Field***

A plot of  $H_{c2}$  versus  $T$  is the same as a plot of  $T_c$  versus  $H$ . Following the distinction of intrinsic and coupling components, there are both intrinsic and coupling upper critical fields. Susceptibility can be used to deduce  $H_{c2}$  versus  $T$  (at high temperatures) in much the same way as it was used to determine  $H_{c1}$  versus  $T$ . At the onset temperature  $T_c$  there is an equivalence between the measuring field and  $H_{c2}$ .<sup>25</sup>

## SUSCEPTOMETER DESIGN

### *Construction*

Low-frequency ac susceptibility measurements are often made with a coaxial mutual-inductance coil system consisting of a primary excitation field coil, a secondary pick-up coil, and a secondary compensation coil (three-coil system). The two secondary coils, connected to a bridge circuit, have the same dimensions. The midpoint between them is concentric with the primary coil.<sup>156-159</sup> An alternative three-coil system, suitable for short or long samples, or when coil length, eddy currents, or temperature gradients are a problem, is with all coils concentric.<sup>160</sup> Here, the pick-up coil is close to the sample, but the compensation and field coils are not. To ensure balance between the pick-up and compensation coils, they are wound so that the mutual inductance of each with respect to the field coil is the same. Another three-coil system uses a large-bore field coil with side-by-side secondary coils.<sup>161</sup> If the compensation coil, or some other field compensation source, is omitted (two-coil system),<sup>162</sup> the measured quantity is ac permeability ( $\mu = \mu' + i\mu''$ ), which is numerically related to ac susceptibility:  $\mu = \mu_0(1 + \chi)$ ,  $\mu' = \mu_0(1 + \chi')$ ,  $\mu'' = \mu_0\chi''$ , where  $\mu_0$  is the permeability of vacuum. If a single coil is used (one-coil system), one can relate the changes in inductance and resistance of the coil to ac  $\chi$ . Calibration is readily achieved in any magnetometric system when the sample is contained within the pick-up coil.

At audio-frequencies, sensitivity is greatest for the susceptometer (three-coil) configuration. The ac susceptometer relies on inductive coupling between coils. A large number of turns on the pick-up coil increases the signal-to-noise ratio at low frequencies but causes capacitive coupling at high frequencies.<sup>163</sup> A typical instrument with 520 turns of 28 gauge wire (0.32 mm diameter) on the primary and 1340 turns of 38 gauge wire (0.10 mm diameter) on each secondary has capacitive coupling above about 5 kHz. The usable frequency range can be extended by reducing the number of turns.<sup>164</sup> Resonance methods, using a single coil<sup>70,165-168</sup> or a two-coil bridge,<sup>169,170</sup> may be used up to radio frequencies. A sample inserted in one of the coils causes a change in self inductance and phase that is related to the susceptibility. These methods are quite sensitive but have been often neglected. For metallic samples, eddy-current signals may present a problem at high frequencies.

Alternating-field susceptibility characterizes the shielding properties of superconductors, whether measured upon cooling or upon warming after zero-field cooling. Typically, measurements are made in zero dc field as a function of ac field or in small ac fields as a function of dc bias field.<sup>89,117,118</sup> The laboratory environment should not be ignored as a source of dc field, particularly in materials, such as sintered high- $T_c$  superconductors, that are weakly coupled. For precise measurements it is desirable to surround the susceptometer with a high-permeability magnetic shield not too close to the coils.

The pick-up and compensation coils may be connected in series opposition or in parallel to the differential input of a lock-in amplifier. The lock-in amplifier may be used either as a null detector upon adjustment of standard inductors and resistors

(Hartshorn bridge),<sup>171</sup> or simply as an off-balance meter. An input band-pass filter should be used to attenuate harmonics with typical attenuation of more than 60 dB. In harmonic susceptibility measurements, filtering is used to isolate the harmonic of interest, as was done in Ref. 89. A constant ac current source (transconductance amplifier) should be used to drive the alternating-field coil if the temperature of the coil changes during the measurement. If the pick-up coil and compensation coil are immersed in liquid helium, Johnson (thermal) noise will be reduced and the coil resistances will remain constant. A disadvantage of this arrangement is that the sample will be weakly coupled to the pick-up coil if a reentrant Dewar is used to control the temperature of the sample. We will describe a system in which the coil temperature changes with that of the sample. To maximize sample coupling, the pick-up coils are wound beneath the field coil. It is generally considered desirable to match the impedance of the pick-up coils to the input impedance of the lock-in amplifier. In practice, however, we have found that there is no advantage in terms of noise or sensitivity, and that the transformer may contribute phase shifts.

Inevitably, there will be mismatch between the pick-up and compensation coils. This can vary with temperature and over time as the coils contract and expand. Two-position susceptometers avoid this problem.<sup>172-177</sup> The sample is measured in each coil, with its position controlled by a sample rod and piston. The voltage signal attributable to the sample changes sign but the signal arising from coil imbalance does not. When the two measurements are subtracted and divided by two, the imbalance signal is removed. To minimize the imbalance and exploit the dynamic range of the lock-in amplifier, we use a trimming loop in series with the field coil. Its position is adjusted once to increase the coupling to either secondary coil. Its contribution to the measurement field is negligible. Sometimes a grounded "coil foil" (a sheet consisting of thin parallel strands of insulated copper wire) is used between the field coil and pick-up coils to reduce their capacitive coupling.<sup>158</sup> We have found that such a shield contributes little to the susceptometer performance. Another possible use for coil foil is for thermal stability.<sup>178</sup>

To help achieve an isothermal environment, we use a sapphire ( $\text{Al}_2\text{O}_3$ ) tube as a coil form. Sapphire is a good thermal conductor and poor electrical conductor. Metal coil forms are not used because they can contribute eddy-current signals. Metal structural components and heaters are well separated from the coils for the same reason. The normal heat leak in the Dewar can be used to slowly warm the sample, or the temperature may be actively controlled. A resistance or semiconductor thermometer and its connecting wires are thermally anchored to the sapphire. (In systems designed for use with high dc bias fields, the thermometer should be relatively insensitive to field. Carbon glass is an example.) Our sample holder is designed in three identical sections so that, in both the upper and lower positions, each secondary coil detects the same holder material except for the sample itself. The holder is open at the sides for sample insertion and removal. The clearance between the sample holder and the sapphire tube is small. To reduce the possibility of damage to the coils from sample-rod motion if air becomes trapped and frozen, we use the release mechanism shown in Fig. 6. The O-ring releases at about 7 N force.

## Phase Adjustment

The phase angle  $\psi$  of the lock-in amplifier used to detect the pick-up coil voltage must be adjusted to correctly separate the real and imaginary parts of susceptibility. The adjustment may be done before the measurement or by computation, after the measurement:  $\chi'_{ext} = \chi'_{ext,0} \cos\psi + \chi''_{ext,0} \sin\psi$ ,  $\chi''_{ext} = \chi''_{ext,0} \cos\psi - \chi'_{ext,0} \sin\psi$ , where the 0 subscripts indicate the measured susceptibilities before adjustment of the phase angle.

Here is an opportunity for the experimentalist to use good judgement. The first guideline is that  $\chi''$  must never be negative. Phase adjustment is accomplished when samples are in low-loss states. Examples are superconductors in the shielding state (low temperature and low measuring field) and spin glasses<sup>179</sup> in the paramagnetic state. Precise phase adjustment is necessary to observe frequency shifts in the susceptibility curves.

The phase adjustment should be repeated for each sample and each measurement frequency but not for each measurement field. It is not practical to adjust phase for each measuring temperature, but, as temperature changes, the resistance of the susceptometer coils does change. This could cause some phase change in the mutual inductance bridge. To avoid this, the lock-in amplifier should be referenced to the voltage drop across a resistor in series with the primary coil.

On the secondary circuit, the input impedance of the lock-in amplifier is large enough to make any change in the coil resistance insignificant. If desired, however, wire with a residual resistivity ratio close to 1, such as brass,<sup>180</sup> could be used to wind the coils instead of copper magnet wire. (Wire with magnetic impurities should be avoided.) An added advantage would be the suppression of any eddy currents in the coils themselves. We have found copper wire to be satisfactory. Phase adjustment at different temperatures may be unavoidable if there are problems with eddy currents in structural elements.

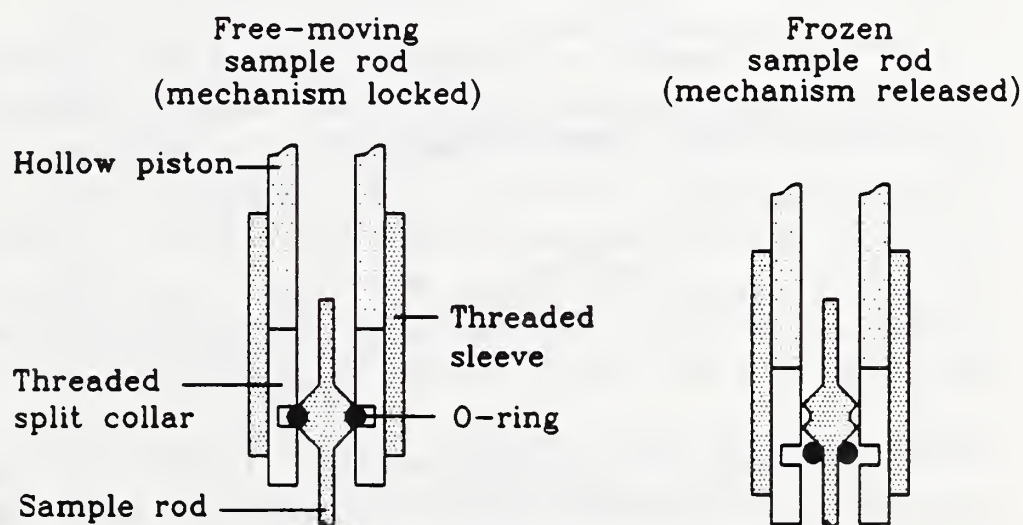


Fig. 6. Release mechanism used to decouple the top of the sample rod from the drive piston if there is excessive resistance to motion. The device is at room temperature, above the experiment Dewar.

## Measurements

With the use of computer controlled instruments, it is tempting to take as much data as possible in a single measurement session. Multiple measurement frequencies may be used at each temperature. It is usually not advisable to change magnetic field strength during the measurement of hysteretic materials because, at high fields, magnetic flux penetrates a superconductor and remains pinned. When measurements are continued at reduced fields, the pinned flux might wiggle around and contribute to the susceptometer signal. For a similar reason, ac measurements are usually best made upon warming, after cooling in zero field. Upon cooling through  $T_c$ , flux exclusion is often incomplete and pinned flux may remain in the sample. The effect is small and it would be of concern only in precise work.

## SUSCEPTOMETER CALIBRATION

### *Analytical and Numerical Calibrations and Standards*

A susceptometer pick-up coil can be calibrated analytically for spherical samples.<sup>156</sup> We use the dipole field of a uniformly magnetized sphere of magnetic moment  $m = MV_s$ , where  $M$  is the magnetization and  $V_s$  is the sample volume, and calculate the total flux  $\Phi$  through a thin pick-up coil of radius  $a$ , length  $\ell$ , and  $n$  turns.<sup>181</sup> We assume  $M = \chi_{ext}H_a$  and  $H_a = H_0 \sin 2\pi ft$ , where  $\chi_{ext}$  is the external susceptibility in SI units and  $H_0$  and  $f$  are the amplitude and frequency of the applied field  $H_a$ . Finally, we use Faraday's law,  $v = d\Phi/dt$ , where  $v$  is the pick-up coil voltage, and get

$$\chi_{ext} = v_{rms} [(\frac{1}{2}\ell)^2 + a^2]^{1/2} / (nV_s\pi f\mu_0 H_{rms}), \quad (39)$$

where we now refer to the rms field and voltage and have ignored any sample voltage induced in the compensation coil. For a given pick-up coil, we assign a constant  $\alpha$  to the quantity  $[(\frac{1}{2}\ell)^2 + a^2]^{1/2} / (n\pi\mu_0)$ . When measuring harmonic susceptibility, the harmonic frequency, not the field frequency, is used for  $f$ .<sup>89</sup>

It is also possible to calibrate susceptometers numerically for cylindrical samples with small susceptibilities ( $\chi \approx 0$ ) or small demagnetizing factors ( $N \approx 0$ ). Either will have almost uniform magnetization. The procedure models the sample as a solenoid and requires computation of the mutual inductance  $L^*$  between the model solenoid and the susceptometer pick-up coil.<sup>182</sup> Once  $L^*$  is known for the sample, we have  $\chi_{ext} = v_{rms} / (L^*\ell 2\pi f H_{rms})$ , where  $v_{rms}$  is the pick-up coil voltage,  $\ell$  is the sample length,  $f$  is the frequency, and  $H_{rms}$  is the applied field. Usually  $L^*$  is calculated numerically, but if the pick-up coil is thin,  $L^*$  can be calculated analytically.<sup>183</sup>

Other calibration methods use standards. These include materials with known susceptibility, and magnetically soft ferromagnets ( $\chi \rightarrow \infty$ ) and superconductors ( $\chi = -1$ ) with known demagnetizing factors (such as spheres and cylinders). These are discussed in Ref. 182. If cylinders are used, accurate values of  $N_m$ , corresponding to the standards' susceptibilities, are necessary.

### Eddy Current Method

A classical exercise is the calculation of the complex magnetic susceptibility of an isotropic, conducting sphere in a uniform ac magnetic field.<sup>184,185</sup> The apparent susceptibility is due to eddy currents, not to the magnetic properties of the material, much like the magnetic susceptibility of a superconductor arises from shielding currents. The real and imaginary parts of external susceptibility are calculated in terms of the sphere radius  $a$  and the skin depth  $\delta$ ,

$$\chi'_{ext} = \frac{9}{4}(\delta/a)[\sinh(2a/\delta) - \sin(2a/\delta)] / [\cosh(2a/\delta) - \cos(2a/\delta)] - \frac{3}{2}, \quad (40a)$$

$$\chi''_{ext} = \frac{9}{4}(\delta/a)[\sinh(2a/\delta) + \sin(2a/\delta)] / [\cosh(2a/\delta) - \cos(2a/\delta)] - \frac{9}{4}(\delta^2/a^2). \quad (40b)$$

In the limit of zero resistivity,  $\delta \rightarrow 0$ ,  $\chi'_{ext} \rightarrow -\frac{3}{2}$ ; using  $N = \frac{1}{3}$  for a sphere,  $\chi' \rightarrow -1$ .

This result provides the basis for another calibration method that uses spheres of normal conductors such as copper. One requirement is knowledge of the temperature dependence of  $\delta$  or, equivalently, resistivity  $\rho$ . Matthiessen's rule, expressed in terms of the residual resistivity ratio  $RRR \equiv \rho(273 \text{ K})/\rho(4 \text{ K})$ , is  $\rho(T) = \rho_i(T) + \rho(273 \text{ K})/RRR$ , where  $\rho_i$  is the intrinsic resistivity. For copper,  $\rho(273 \text{ K}) = 1.543 \times 10^{-8} \Omega \cdot \text{m}$ , and values of RRR range from 10 to 2000. Values of  $\rho_i(T)$  are tabulated.<sup>186</sup> From  $\rho(T)$  we calculate  $\delta(T) = [\rho(T)/(\pi f \mu)]^{1/2}$ , where  $f$  is the measurement frequency and  $\mu = \mu_0$  for a nonmagnetic material. The point is that a copper sphere with known RRR will have predictable curves of  $\chi'_{ext}$  and  $\chi''_{ext}$  (or  $\chi'$  and  $\chi''$ ) as functions of temperature and frequency. [If the ac susceptometer is already calibrated, this method can be used to measure  $\rho(T)$ .] In Fig. 7 we show  $\chi'_{ext}$  and  $\chi''_{ext}$  as functions of temperature for a copper sphere,  $a = 3.088 \text{ mm}$ , at 10, 100, and 1000 Hz (points). The measurement field was  $80 \text{ A} \cdot \text{m}^{-1}$  rms, although the susceptibilities are independent of field. The curves shown are the predicted  $\chi'_{ext}$  and  $\chi''_{ext}$  from the

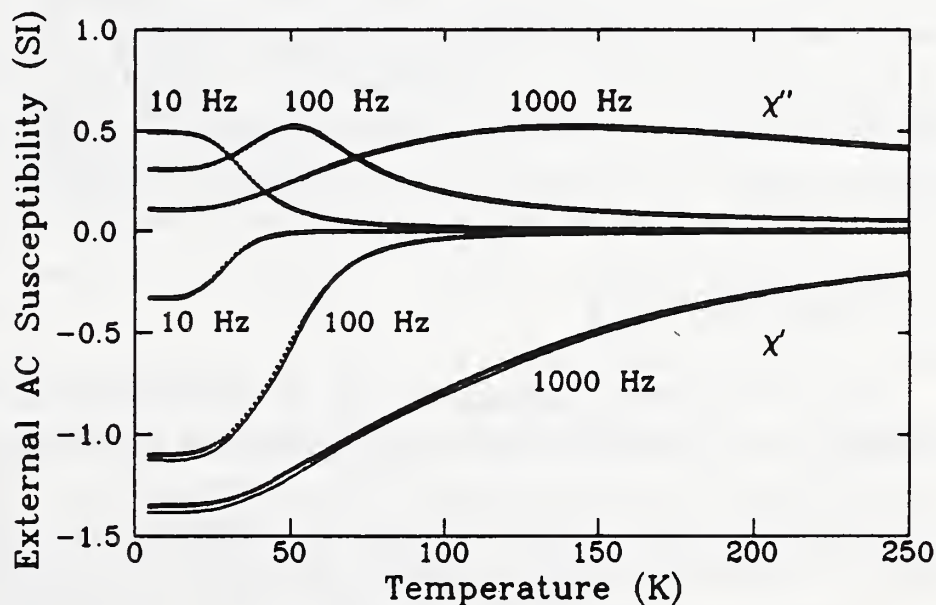


Fig. 7. Apparent susceptibility of a copper sphere as a function of temperature at 10, 100, and 1000 Hz based on eddy currents and skin depth. Points are measured susceptibilities; curves are calculated susceptibilities.

eddy-current equations. The curves overlap the data at 10 Hz. The adjustable parameters were the lock-in-amplifier phase angle  $\psi$  (for each frequency) and RRR (adjusted to 150). We have used the 1000-Hz data in lectures to show students an “onset of diamagnetism” near 300 K: a room-temperature superconductor!

Two related problems are for infinite cylinders in perpendicular and parallel fields.<sup>146,164,184,187–191</sup> The infinite-cylinder solutions, together with the demagnetizing factors in Table 1, suggest that calibrations can be done with finite-sized cylinders provided  $\delta$  is small (that is,  $\rho$  is small and  $f$  is large).

## SUSCEPTOMETER SENSITIVITY

The equation that describes the response of an ac susceptometer is  $\chi_{ext} = \alpha v / (V_s f H_a)$ , where  $\chi_{ext}$  is the volume susceptibility in SI units,  $\alpha$  is the calibration constant (a function of the pick-up coil geometry) [ $\text{A} \cdot \text{m}^2 \cdot \text{V}^{-1} \cdot \text{s}^{-1}$ ],  $v$  is the pick-up coil voltage [V],  $V_s$  is the sample volume [ $\text{m}^3$ ],  $f$  is the frequency [ $\text{s}^{-1}$ ], and  $H_a$  is the magnetic field strength [ $\text{A} \cdot \text{m}^{-1}$ ]. The sensitivity of an ac susceptometer depends on  $\alpha$  and on the precision in the output  $v_p$  of the ac voltmeter, typically a lock-in amplifier. Usually  $v$  is proportional to  $f$ , so  $\alpha v_p / f$  is the magnetic moment precision [ $\text{A} \cdot \text{m}^2$ ]. (There is actually some degradation in voltage precision  $v_p$  at low frequencies such as 10 Hz due to  $1/f$  noise.) For one of our susceptometers,  $\alpha = 2.1546$  and  $v_p / f = 2.5 \times 10^{-10}$ , giving a moment precision of  $5 \times 10^{-10} \text{ A} \cdot \text{m}^2$  ( $5 \times 10^{-7}$  emu). For comparison, commercial vibrating-sample magnetometers are able to measure about  $5 \times 10^{-8} \text{ A} \cdot \text{m}^2$  ( $5 \times 10^{-5}$  emu) and commercial SQUID magnetometers can detect about  $10^{-11} \text{ A} \cdot \text{m}^2$  ( $10^{-8}$  emu). In principle, their sensitivity can be improved by increasing the pick-up coils' filling factor.<sup>192,193</sup> Alternating-gradient-force magnetometers can measure about  $10^{-11} \text{ A} \cdot \text{m}^2$  ( $10^{-8}$  emu).<sup>194</sup>

Our moment precision of  $5 \times 10^{-10} \text{ A} \cdot \text{m}^2$  means the precision in  $\chi_{ext}$  is  $5 \times 10^{-10} / (V_s H)$ . (That is, we can measure the susceptibility of a sample more precisely if we have a larger sample or use a larger measuring field.) For the favorable case of a sample sphere of diameter 5 mm measured in a field of  $800 \text{ A} \cdot \text{m}^{-1}$ , the susceptibility precision would be  $10^{-5}$  (SI). For a 3-mm-diameter sphere measured in  $80 \text{ A} \cdot \text{m}^{-1}$ , the precision would be only  $4 \times 10^{-4}$  (SI). This assumes that both  $V_s$  and  $H$  are known exactly. Precision is not the same as accuracy, which depends on instrument calibration.

## ACKNOWLEDGMENTS

We had valuable discussions with D.-X. Chen (Universitat Autònoma de Barcelona), I. B. Goldberg (Rockwell International Corporation), T. Ishida (Ibaraki University), and J. K. Krause (Lake Shore Cryotronics, Inc.). R. A. Hein (University of Washington) offered many thoughtful comments and suggestions. A sintered Y–Ba–Cu–O sample was provided by A. K. Mehrotra. D. L. Ried, R. L. Spomer, and R. J. Loughran assisted with data acquisition. T. W. Petersen, R. M. Gerrans, and R. W. Cross prepared the figures for publication. Work at the National Institute of Standards and Technology was supported by the Electronics and Electrical Engineering Laboratory. This paper is not subject to copyright.

## REFERENCES

1. W. Thomson, "Reprint of Papers on Electrostatics and Magnetism," Macmillan and Co., London (1872), p. 472.
2. In his original paper, *Phil. Mag.*, ser. 4, 1:177 (1851), Thomson used the term "inductive capacity" for susceptibility, which seems to associate susceptibility with the magnetic induction  $B$ . He abandoned this term by 1872, possibly on the suggestion of Maxwell. Maxwell used the term "magnetic inductive capacity" for permeability in "A Treatise on Electricity and Magnetism," first published in 1873.
3. W. Meissner and R. Ochsenfeld, *Naturwissenschaften* 21:787 (1933).
4. R. A. Hein, *Phys. Rev. B* 33:7539 (1986).
5. D. Shoenberg, "Superconductivity," Cambridge University Press, Cambridge, U.K. (1962), pp. 43-47.
6. F. G. A. Tarr and J. O. Wilhelm, *Can. J. Res.* 12:265 (1935).
7. D. Shoenberg, *Proc. Cambridge Phil. Soc.* 33:260 (1937).
8. P. B. Alers, J. W. McWhirter, and C. F. Squire, in: "Low-Temperature Physics," Nat. Bur. Stand. (U.S.), Circular 519 (1952), p. 85-88.
9. M. B. Elzinga and C. Uher, *Phys. Rev. B* 32:88 (1985).
10. R. A. Hein and R. L. Falge, Jr., *Phys. Rev.* 123:407 (1961).
11. L. Krusin-Elbaum, A. P. Malozemoff, and Y. Yeshurun, in: "High-Temperature Superconductors," M. B. Brodsky, R. C. Dynes, K. Kitazawa, and H. L. Tuller, eds., Materials Research Society, Pittsburgh, *Symp. Proc.* 99:221 (1988).
12. L. Krusin-Elbaum, A. P. Malozemoff, Y. Yeshurun, D. C. Cronmeyer, and F. Holtzberg, *Physica C* 153-155:1469 (1988).
13. V. I. Aleksandrov, M. A. Borik, V. G. Veselago, V. V. Voronov, Yu. K. Voron'ko, P. A. Ivanov, G. V. Maksimova, V. E. Makhotkin, V. A. Myzina, V. V. Osiko, A. M. Prokhorov, V. M. Tatarintsev, V. T. Udovenchik, V. A. Fradkov, and M. A. Chernikov, *JETP Lett. (Suppl.)* 46:S77 (1987) [*Pis'ma Zh. Eksp. Teor. Fiz. (Prilozh.)* 46:90 (1987)].
14. V. V. Alexandrov, V. V. Borisovskii, T. A. Fedotova, L. M. Fisher, N. V. Il'in, O. K. Smirnova, I. F. Voloshin, M. A. Baranov, and V. S. Gorbachev, *Physica C* 173:458 (1991).
15. S. Ruppel, G. Michels, H. Geus, J. Kalenborn, W. Schlabit, B. Roden, and D. Wohlleben, *Physica C* 174:233 (1991).
16. M. Tinkham, "Introduction to Superconductivity," Krieger Publishing, Malabar, Florida (1980), pp. 244-250.
17. R. B. Goldfarb, A. F. Clark, A. I. Braginski, and A. J. Panson, *Cryogenics* 27:475 (1987).
18. D.-X. Chen, R. B. Goldfarb, J. Nogués, and K. V. Rao, *J. Appl. Phys.* 63:980 (1988).
19. D.-X. Chen, J. Nogués, N. Karpe, and K. V. Rao, *Kexue Tongbao* (Beijing, English edition) 33:560 (1988).
20. H. Mazaki, M. Takano, R. Kanno, and Y. Takeda, *Jpn. J. Appl. Phys.* 26:L780 (1987).
21. T. Ishida and H. Mazaki, *Jpn. J. Appl. Phys.* 26:L1296 (1987).
22. H. Mazaki, M. Takano, Y. Ikeda, Y. Bando, R. Kanno, Y. Takeda, and O. Yamamoto, *Jpn. J. Appl. Phys.* 26:L1749 (1987).
23. J. García, C. Rillo, F. Lera, J. Bartolomé, R. Navarro, D. H. A. Blank, and J. Flokstra, *J. Magn. Magn. Mater.* 69:L225 (1987).
24. R. Renker, I. Apfelstedt, H. Küpfer, C. Politis, H. Rietschel, W. Schauer, H. Wühl, U. Gottwick, H. Kneissel, U. Rauchschalbe, H. Spille, and F. Steglich, *Z. Phys. B* 67:1 (1987).

25. H. Küpfer, I. Apfelstedt, W. Schauer, R. Flükiger, R. Meier-Hirmer, and H. Wühl, *Z. Phys. B* **69**:159 (1987).
26. J. R. Cave, A. Février, Hoang Gia Ky, and Y. Laumond, *IEEE Trans. Magn.* **23**:1732 (1987).
27. C. M. Bastuscheck, R. A. Buhrman and J. C. Scott, *Phys. Rev. B* **24**:6707 (1981).
28. C. Ebner and D. Stroud, *Phys. Rev. B* **31**:165 (1985).
29. P. England, F. Goldie, and A. D. Caplin, *J. Phys. F: Met. Phys.* **17**:447 (1987).
30. Y. M. Chiang, J. A. S. Ikeda, and A. Roshko, in: "Ceramic Superconductors II," M. F. Yan, ed., American Ceramics Society, Westerville, Ohio (1988), p. 607.
31. S. E. Babcock, T. F. Kelly, P. J. Lee, J. M. Seuntjens, L. A. Layanier, and D. C. Larbalestier, *Physica C* **152**:25 (1988).
32. P. Dubots and J. Cave, *Cryogenics* **28**:661 (1988).
33. D. K. Finnemore, R. N. Shelton, J. R. Clem, R. W. McCallum, H. C. Ku, R. E. McCarley, S. C. Chen, P. Klavins, and V. Kogan, *Phys. Rev. B* **35**:5319 (1987).
34. J. W. Ekin, A. I. Braginski, A. J. Panson, M. A. Janocko, D. W. Capone II, N. J. Zaluzec, B. Flandermeyer, O. F. de Lima, M. Hong, J. Kwo, and S. H. Liou, *J. Appl. Phys.* **62**:4821 (1987).
35. M. Suenaga, A. Ghosh, T. Asano, R. L. Sabatini, and A. R. Moodenbaugh, in: "High Temperature Superconductors," D. U. Gubser and M. Schluter, eds., Materials Research Society, Pittsburgh, **EA-11**:247 (1987).
36. D. C. Larbalestier, M. Daeumling, X. Cai, J. Seuntjens, J. McKinnell, D. Hampshire, P. Lee, C. Meingast, T. Willis, H. Muller, R. D. Ray, R. G. Dillenburg, E. E. Hellstrom, and R. Joynt, *J. Appl. Phys.* **62**, 3308 (1987).
37. T. Ishida and H. Mazaki, *J. Appl. Phys.* **52**:6798 (1981).
38. T. Ishida, K. Kanoda, H. Mazaki, and I. Nakada, *Phys. Rev. B* **29**:1183 (1984).
39. H. Mazaki and T. Ishida, *Jpn. J. Appl. Phys.* **26**:L1508 (1987).
40. Y. Oda, I. Nakada, T. Kohara, H. Fujita, T. Kaneko, H. Toyoda, E. Sakagami, and K. Asayama, *Jpn. J. Appl. Phys.* **26**:L481 (1987).
41. E. Babić, Ž. Marohnić, Đ. Drobac, M. Prester, and N. Brničević, *Physica C* **153-155**: 1511 (1988).
42. H. M. Ledbetter, S. A. Kim, R. B. Goldfarb, and K. Togano, *Phys. Rev. B* **39**:9689 (1989).
43. The material described in Fig. 2 was used in an interlaboratory comparison sponsored by the Defense Advanced Research Projects Agency (DARPA) in 1989. Participants were asked to determine  $T_c$  by susceptibility and report "the midpoint of the full inductive transition," presumably referring to the coupling transition. No guidance was given as to measuring field. The 16 participants reported  $T_c$ 's ranging from 83 to 94 K. Most of the systematic differences in the measurements were likely due to different measuring fields used by the participants.
44. X. Obradors, C. Rillo, M. Vallet, A. Labarta, J. Fontcuberta, J. Gonzalez-Calbet, and F. Lera, *Physica C* **153-155**:389 (1988).
45. H. Morita, K. Watanabe, Y. Murakami, S. Kondo, Y. Obi, K. Noto, H. Fujimori, and Y. Muto, *Physica B* **148**:449 (1987).
46. H. Nobumasa, K. Shimizu, Y. Kitano, and T. Kawai, *Jpn. J. Appl. Phys.* **27**:L846 (1988).
47. C. E. Gough, *J. Physique Colloq.* **49**:C8-2075 (1988).
48. A. K. Sarkar, B. Kumar, I. Maartense, and T. L. Peterson, *J. Appl. Phys.* **65**:2392 (1989).
49. A. Mehdaoui, B. Loegel, and D. Bolmont, *J. Appl. Phys.* **66**:1497 (1989).
50. E. C. Stoner, *Phil. Mag.*, ser. 7, **36**:803 (1945).
51. J. A. Osborn, *Phys. Rev.* **67**:351 (1945).
52. D.-X. Chen, J. A. Brug, and R. B. Goldfarb, *IEEE Trans. Magn.* **27**:3601 (1991).

53. T. T. Taylor, *J. Res. Nat. Bur. Stand. (U.S.)* **64B**:199 (1960).
54. D.-X. Chen, "Physical Basis of Magnetic Measurements," China Mechanical Industry, Beijing (1985), pp. 139-140.
55. S. D. Murphy, K. Renouard, R. Crittenden, and S. M. Bhagat, *Solid State Commun.* **69**:367 (1989).
56. J. Ferreirinho, S. J. Lee, S. J. Campbell, and A. Calka, *J. Magn. Magn. Mater.* **88**:281 (1990).
57. J. Clerk Maxwell, "A Treatise on Electricity and Magnetism," 3rd Ed., Vol. 2, Clarendon Press, Oxford (1892), pp. 57-58 and pp. 476-477. Reprinted, Dover Publications, New York (1954).
58. A. M. Campbell, F. J. Blunt, J. D. Johnson, and P. A. Freeman, *Cryogenics* **31**:732 (1991).
59. R. Navarro and L. J. Campbell, unpublished, 1991.
60. T. C. Choy and A. M. Stoneham, *J. Phys.: Condens. Matter* **2**:939 (1990).
61. J. R. Clem and V. G. Kogan, *Jpn. J. Appl. Phys. Suppl.* **26-3**:1161 (1987).
62. T. Ishida and H. Mazaki, *Jpn. J. Appl. Phys.* **26**:L2003 (1987).
63. G. Aeppli, R. J. Cava, E. J. Ansaldo, J. H. Brewer, S. R. Kreitzman, G. M. Luke, D. R. Noakes, and R. F. Kiefl, *Phys. Rev. B* **35**:7129 (1987).
64. Y. J. Uemura, V. J. Emery, A. R. Moodenbaugh, M. Suenaga, D. C. Johnston, A. J. Jacobson, J. T. Lewandowski, J. H. Brewer, R. F. Kiefl, S. R. Kreitzman, G. M. Luke, T. Riseman, C. E. Stronach, W. J. Kossler, J. R. Kempton, X. H. Yu, D. Opie, and H. Schone, *Phys. Rev. B* **38**:909 (1988).
65. J. R. Cooper, C. T. Chu, L. W. Zhou, B. Dunn, and G. Grüner, *Phys. Rev. B* **37**:638 (1988).
66. R. J. Cava, B. Batlogg, R. B. van Dover, D. W. Murphy, S. Sunshine, T. Siegrist, J. P. Remeika, E. A. Rietman, S. Zahurak, and G. P. Espinosa, *Phys. Rev. Lett.* **58**:1698 (1987).
67. P. M. Grant, R. B. Beyers, E. M. Engler, G. Lim, S. S. P. Parkin, M. L. Ramirez, V. Y. Lee, A. Nazzal, J. E. Vasquez, and R. J. Savoy, *Phys. Rev. B* **35**:7242 (1987).
68. A. J. Panson, A. I. Braginski, J. R. Gavaler, J. K. Hulm, M. A. Janoko, H. C. Pohl, A. M. Stewart, J. Talvacchio, and G. R. Wagner, *Phys. Rev. B* **35**:8874 (1987).
69. A. C. Rose-Innes and E. H. Rhoderick, "Introduction to Superconductivity," 2nd Ed., Pergamon Press, Oxford, U.K. (1978), p. 93-97.
70. A. L. Schawlow and G. E. Devlin, *Phys. Rev.* **113**:120 (1959).
71. D.-X. Chen, Y. Mei, and H. L. Luo, *Physica C* **167**:317 (1990).
72. D.-X. Chen, A. Sánchez, T. Puig, L. M. Martínez, and J. S. Muñoz, *Physica C* **168**:652 (1990).
73. Ref. 57, p. 70. Maxwell probably meant to refer to Art. 429 in this quotation.
74. R. B. Goldfarb, *Cryogenics* **26**:621 (1986).
75. J. A. Cape and J. M. Zimmerman, *Phys. Rev.* **153**:416 (1967).
76. L. D. Landau, E. M. Lifshitz, and L. P. Pitaevskii, "Electrodynamics of Continuous Media," 2nd Ed., Pergamon Press, Oxford, U.K. (1984), p. 185.
77. V. F. Elesin, I. V. Zakharchenko, A. A. Ivanov, A. P. Menushenkov, A. A. Sinchenko, and S. V. Shavkin, *Supercond., Phys. Chem. Technol.* **3**:1376 (1990) [*Sverkhprovodn., Fiz. Khim. Tekh.* **3**: 1704 (1990)].
78. P. G. de Gennes, "Superconductivity of Metals and Alloys," Addison-Wesley, Redwood City, California (1989), pp. 60-63.
79. E. M. Gyorgy, *AT&T Bell Laboratories*, personal communication, 1990.
80. H. Teshima, A. Oishi, H. Izumi, K. Ohata, T. Morishita, and S. Tanaka, *Appl. Phys. Lett.* **58**:2833 (1991).
81. J. A. Agostinelli, G. R. Paz-Pujalt, and A. K. Mehrotra, *Physica C* **156**:1208 (1988).

82. M. Leleental, S. Chen, S.-Tong Lee, G. Braunstein, and T. Blanton, *Physica C* **167**:614 (1990).
83. D. Majumdar and M. Leleental, *Physica C* **161**:145 (1989).
84. T. Blanton, M. Leleental, C. L. Barnes, *Physica C* **173**:152 (1991).
85. R. B. Goldfarb, Magnetic units and material specification, in: "Concise Encyclopedia of Magnetic and Superconducting Materials," J. E. Evetts, ed., Pergamon Press, Oxford, U.K. (1992).
86. C. P. Bean, *Rev. Mod. Phys.* **36**:31 (1964).
87. H. London, *Phys. Lett.* **6**:162 (1963).
88. Y. B. Kim, C. F. Hempstead, and A. R. Strnad, *Phys. Rev.* **129**:528 (1963).
89. T. Ishida and R. B. Goldfarb, *Phys. Rev. B* **41**:8939 (1990).
90. D.-X. Chen and R. B. Goldfarb, *J. Appl. Phys.* **66**:2489 (1989).
91. Ref. 76, pp. 204-205.
92. J. R. Clem, "AC Losses in Type-II Superconductors," Ames Lab. Tech. Rep. IS-M 280, Iowa State University, Ames, Iowa (1979), Eqs. (25). Reprinted with additions in: "Magnetic Susceptibility of Superconductors and Other Spin Systems," R. A. Hein, T. L. Francavilla, and D. H. Liebenberg, eds., Plenum Press, New York (1992).
93. C. P. Bean, *Rev. Mod. Phys.* **36**:31 (1964).
94. These slab equations for  $\chi'$  and  $\chi''$  may be obtained by simplification of Eqs. (9) in: L. Ji, R. H. Sohn, G. C. Spalding, C. J. Lobb, and M. Tinkham, *Phys. Rev. B* **40**:10936 (1989).
95. C. P. Bean, *Phys. Rev. Lett.* **8**:250 (1962).
96. W. A. Fietz and W. W. Webb, *Phys. Rev.* **178**:657 (1969).
97. These axial cylinder equations for  $\chi'$  and  $\chi''$  may be obtained by simplification of Eqs. (118)–(124) in Ref. 92. Note that  $2 \sin^{-1}(x^{-1/2}) = \cos^{-1}(1 - 2/x)$ .
98. R. B. Goldfarb and A. F. Clark, *IEEE Trans. Magn.* **21**:332 (1985).
99. W. J. Carr, Jr., M. S. Walker, and J. H. Murphy, *J. Appl. Phys.* **46**:4048 (1975).
100. W. J. Carr, Jr., J. H. Murphy, and G. R. Wagner, *Adv. Cryo. Eng.* **24**:415 (1978).
101. W. J. Carr, Jr. and G. R. Wagner, *Adv. Cryo. Eng. (Materials)* **30**:923 (1984).
102. W. J. Carr, Jr., "AC Loss and Macroscopic Theory of Superconductors," Gordon and Breach, New York (1983), pp. 63-67.
103. M. Ashkin, *J. Appl. Phys.* **50**:7060 (1979).
104. V. B. Zenkevitch, A. S. Romanyuk, and V. V. Zheltov, *Cryogenics* **20**:703 (1980).
105. C. Y. Pang, P. G. McLaren, and A. M. Campbell, *Int. Cryo. Eng. Conf.* **8**:739 (1980).
106. J. V. Minervini, *Adv. Cryo. Eng. (Materials)* **28**:587 (1982).
107. M. N. Wilson, "Superconducting Magnets," Clarendon Press, Oxford, U.K. (1983), pp. 165-170.
108. K. V. Bhagwat and P. Chaddah, *Physica C* **166**:1 (1990).
109. J. W. Ekin, *Appl. Phys. Lett.* **55**:905 (1989).
110. D. M. Kroeger, C. C. Koch, and J. P. Charlesworth, *J. Low Temp. Phys.* **19**:493 (1975).
111. R. B. Goldfarb and A. F. Clark, *J. Appl. Phys.* **57**:3809 (1985).
112. J. R. Cave, P. R. Critchlow, P. Lambert, and B. Champagne, *IEEE Trans. Magn.* **27**:1379 (1991).
113. J. R. Clem, *Physica C* **153-155**:50 (1988).
114. J. Z. Sun, M. J. Scharen, L. C. Bourne, and J. R. Schrieffer, *Phys. Rev. B* **44**:5275 (1991).
115. F. Gömöry and P. Lobotka, *Solid State Commun.* **66**:645 (1988).
116. D.-X. Chen, J. Nogués, and K. V. Rao, *Cryogenics* **29**:800 (1989).
117. A. M. Campbell, *J. Phys. C: Solid State Phys.* **2**:1492 (1969).

118. R. W. Rollins, H. Küpfer, and W. Gey, *J. Appl. Phys.* **45**:5392 (1974).
119. H. Küpfer, I. Apfelstedt, R. Flükiger, C. Keller, R. Meier-Hirmer, B. Runtsch, A. Turowski, U. Wiech, and T. Wolf, *Cryogenics* **29**:268 (1989).
120. H. A. Ullmaier, *Phys. Stat. Sol.* **17**:631 (1966).
121. D. M. Kroeger, C. C. Koch, and W. A. Coghlan, *J. Appl. Phys.* **44**:2391 (1973).
122. A. Shaulov and D. Dorman, *Appl. Phys. Lett.* **53**:2680 (1988).
123. E. M. Gyorgy, R. B. van Dover, K. A. Jackson, L. F. Schneemeyer, and J. V. Waszczak, *Appl. Phys. Lett.* **55**:283 (1989).
124. R. L. Peterson, *J. Appl. Phys.* **67**:6930 (1990).
125. C. P. Bean and J. D. Livingston, *Phys. Rev. Lett.* **12**:14 (1964).
126. R. W. Rollins and J. Silcox, *Phys. Rev.* **155**:404 (1967).
127. D.-X. Chen, R. W. Cross, and A. Sánchez, unpublished, 1991.
128. S. A. Campbell, J. B. Ketterson, and G. W. Crabtree, *Rev. Sci. Instrum.* **54**:1191 (1983).
129. B. Loegel, A. Mehdaoui, and D. Bolmont, *Supercond. Sci. Technol.* **3**:504 (1990).
130. R. W. Cross and R. B. Goldfarb, *J. Appl. Phys.* **67**:5476 (1990).
131. J. R. Clem, *J. Appl. Phys.* **50**, 3518 (1979).
132. R. B. Goldfarb, A. F. Clark, A. J. Panson, and A. I. Braginski, in: "High Temperature Superconductors," D. U. Gubser and M. Schluter, eds., Materials Research Society, Pittsburgh, EA-11:261 (1987).
133. R. J. Loughran and R. B. Goldfarb, *Physica C* **181**:138 (1991).
134. E. Babić, Ž. Marohnić, Đ. Drobac, and M. Prester, *Int. J. Mod. Phys. B* **1**:973 (1987).
135. M. Avirovic, Ch. Neumann, P. Ziemann, J. Geerk, and H. C. Li, *Solid State Commun.* **67**:795 (1988).
136. L. Krusin-Elbaum, A. P. Malozemoff, Y. Yeshurun, D. C. Cronmeyer, and F. Holtzberg, *Phys. Rev. B* **39**:2936 (1989).
137. V. V. Moshchalkov, J. Y. Henry, C. Marin, J. Rossat-Mignod, and J. F. Jacquot, *Physica C* **175**:407 (1991).
138. E. W. Collings, A. J. Markworth, J. K. McCoy, K. R. Marken, Jr., M. D. Sumption, E. Gregory, and T. S. Kreilick, *Adv. Cryo. Eng. (Materials)* **36**:255 (1990).
139. S. Takács, *Czech. J. Phys. B* **33**:1248 (1983).
140. K.-H. Müller, *Physica C* **159**:717 (1989).
141. R. B. Goldfarb and R. L. Spomer, *Adv. Cryo. Eng. (Materials)* **36**:215 (1990).
142. M. Nikolo and R. B. Goldfarb, *Phys. Rev. B* **39**:6615 (1989).
143. T. T. M. Palstra, B. Batlogg, R. B. van Dover, L. F. Schneemeyer, and J. V. Waszczak, *Phys. Rev. B* **41**:6621 (1990).
144. J. H. P. M. Emmen, V. A. M. Brabers, and W. J. M. de Jonge, *Physica C* **176**:137 (1991).
145. E. Maxwell and M. Strongin, *Phys. Rev. Lett.* **10**:212 (1963).
146. G. D. Cody and R. E. Miller, *Phys. Rev.* **173**:481 (1968).
147. L. M. Fisher, N. V. Il'yn, and I. F. Voloshin, *Adv. Cryo. Eng. (Materials)* **36**:423 (1990).
148. F. Irie and K. Yamafuji, *J. Phys. Soc. Jpn.* **23**:255 (1967).
149. J. R. Clem, H. R. Kerchner, and S. T. Sekula, *Phys. Rev. B* **14**:1893 (1976).
150. S. Takács, F. Gömörý, and P. Lobotka, *IEEE Trans. Magn.* **27**:1057 (1991).
151. A. F. Khoder, *Phys. Lett.* **94A**:378 (1983).
152. A. F. Khoder, M. Couach, and B. Barbara, *Physica C* **153-155**:1477 (1988).
153. C. Lucchini, C. Giovannella, R. Messi, B. Lecuyer, L. Fruchter, and M. Iannuzzi, *Phys. Stat. Sol. B* **157**: K123 (1990).
154. A. Gianelli and C. Giovannella, *Physica A* **168**:277 (1990).

155. R. A. Hein, H. Hojaji, A. Barkatt, H. Shafii, K. A. Michael, A. N. Thorpe, M. F. Ware, and S. Alterescu, *J. Supercond.* **2**:427 (1989).
156. W. R. Abel, A. C. Anderson, and J. C. Wheatley, *Rev. Sci. Instrum.* **43**:444 (1964).
157. W. L. Pillinger, P. S. Jastram, and J. G. Daunt, *Rev. Sci. Instrum.* **29**:159 (1958).
158. S. C. Whitmore, S. R. Ryan, and T. M. Sanders, *Rev. Sci. Instrum.* **49**:1579 (1978).
159. J. R. Owers-Bradley, Wen-Sheng Zhou, and W. P. Halperin, *Rev. Sci. Instrum.* **52**:1106 (1981).
160. D.-X. Chen, "Ballistic and Bridge Methods of Magnetic Measurements of Materials," China Metrology, Beijing (1990), pp. 526-572.
161. Ref. 107, pp. 243-249.
162. D. Shoenberg, *Proc. Cambridge Phil. Soc.* **33**:559 (1937).
163. P. H. Müller, M. Schienle, and A. Kasten, *J. Magn. Magn. Mater.* **28**:341 (1982).
164. T. Ishida, K. Monden, and I. Nakada, *Rev. Sci. Instrum.* **57**:3081 (1986).
165. B. J. Dalrymple and D. E. Prober, *Rev. Sci. Instrum.* **55**:958 (1984).
166. D. G. Xenikos and T. R. Lemberger, *Rev. Sci. Instrum.* **60**:831 (1989).
167. J. N. Fox and J. U. Trefny, *Am. J. Phys.* **43**:622 (1975).
168. J. G. Elliott and W. Y. Liang, *Meas. Sci. Technol.* **1**:1351 (1990).
169. I. Maartense, *Rev. Sci. Instrum.* **41**:657 (1970).
170. I. Maartense, *J. Appl. Phys.* **53**:2466 (1982).
171. L. Hartshorn, *J. Sci. Instrum.* **2**:145 (1925).
172. A. J. de Vries and J. W. M. Livius, *Appl. Sci. Res.* **17**:31 (1967).
173. H. A. Groenendijk, A. J. van Duyneveldt, and R. D. Willett, *Physica B* **101**:320 (1980).
174. J. L. Tholence, F. Holtzberg, T. R. McGuire, S. von Molnar, and R. Tournier, *J. Appl. Phys.* **50**:7350 (1979).
175. A. J. van Duyneveldt, *J. Appl. Phys.* **53**:8006 (1982).
176. A. F. Deutz, R. Hulstman, and F. J. Kranenburg, *Rev. Sci. Instrum.* **60**:113 (1989).
177. A. K. Rastogi, *Jawaharlal Nehru University, New Delhi*, and J. L. Tholence, *Centre National de la Recherche Scientifique, Grenoble*, personal communication, 1985.
178. L. J. de Jongh, W. D. van Amstel, and A. R. Miedema, *Physica* **58**:277 (1972).
179. K. Baberschke, *Freie Universität Berlin*, personal communication, 1984.
180. F. R. Fickett, in: "Materials at Low Temperatures," R. P. Reed and A. F. Clark, eds., American Society for Metals, Metals Park, Ohio (1983), pp. 164-165.
181. The flux from an *ellipsoidal* sample through a *single-turn* pick-up coil is calculated in: M. Denhoff, S. Gyax, and J. R. Long, *Cryogenics* **21**:400 (1981).
182. R. B. Goldfarb and J. V. Minervini, *Rev. Sci. Instrum.* **55**:761 (1984). On page 763, second column, line 3 and Fig. 3, " $L^*$ " should be " $2L^*$ ."
183. L. Cohen, *Bull. Bureau Standards* **3**:295 (1907).
184. Ref. 76, pp. 205-207.
185. J. E. Zimmerman, *Rev. Sci. Instrum.* **32**:402 (1961).
186. R. A. Matula, *J. Phys. Chem. Ref. Data* **8**:1147 (1979).
187. R. M. Bozorth, "Ferromagnetism," Van Nostrand, Princeton, New Jersey (1951), pp. 775-776.
188. R. G. Chambers and J. G. Park, *Brit. J. Appl. Phys.* **12**:507 (1961).
189. M. D. Rosenthal and B. W. Maxfield, *Rev. Sci. Instrum.* **46**:398 (1975).
190. A. M. Ricca and S. Zannella, *IEEE Trans. Magn.* **23**:1422 (1987).
191. H. Zijlstra, "Experimental Methods in Magnetism," Vol. 2, North-Holland, Amsterdam (1967), pp. 72-79.
192. S. Foner, *Rev. Sci. Instrum.* **46**:1425 (1975).
193. J. S. Philo and W. M. Fairbank, *Rev. Sci. Instrum.* **48**:1529 (1977).
194. P. J. Flanders, *J. Appl. Phys.* **63**:3940 (1988).

BL-114A (5-90)  <b>BIBLIOGRAPHIC DATA SHEET</b>	<b>U.S. DEPARTMENT OF COMMERCE</b> <b>NATIONAL INSTITUTE OF STANDARDS AND TECHNOLOGY</b>		1. PUBLICATION OR REPORT NUMBER NISTIR 3977
			2. PERFORMING ORGANIZATION REPORT NUMBER B92-0009
			3. PUBLICATION DATE October 1991
4. TITLE AND SUBTITLE Alternating-Field Susceptometry and Magnetic Susceptibility of Superconductors			
5. AUTHOR(S) R. B. Goldfarb, M. Lelental, and C. A. Thompson			
6. PERFORMING ORGANIZATION (IF JOINT OR OTHER THAN NIST, SEE INSTRUCTIONS) U.S. DEPARTMENT OF COMMERCE NATIONAL INSTITUTE OF STANDARDS AND TECHNOLOGY BOULDER, COLORADO 80303-3328		7. CONTRACT/GRANT NUMBER	8. TYPE OF REPORT AND PERIOD COVERED
9. SPONSORING ORGANIZATION NAME AND COMPLETE ADDRESS (STREET, CITY, STATE, ZIP)			
10. SUPPLEMENTARY NOTES  Published in: "Magnetic Susceptibility of Superconductors and Other Spin Systems," R. A. Hein, T. L. Francavilla, and D. H. Liebenberg, Editors, Plenum Press, New York (1992).			
11. ABSTRACT (A 200-WORD OR LESS FACTUAL SUMMARY OF MOST SIGNIFICANT INFORMATION. IF DOCUMENT INCLUDES A SIGNIFICANT BIBLIOGRAPHY OR LITERATURE SURVEY, MENTION IT HERE.)  <p>This review critically analyzes current practice in the design, calibration, sensitivity determination, and operation of alternating-field susceptometers, and examines applications in magnetic susceptibility measurements of superconductors. Critical parameters of the intrinsic and coupling components of granular superconductors may be deduced from magnetic susceptibility measurements. The onset of intrinsic diamagnetism corresponds to the initial decrease in electrical resistivity upon cooling, but the onset of intergranular coupling coincides with the temperature for zero resistivity. The lower critical field may be determined by the field at which the imaginary part of susceptibility increases from zero. Unusual features in the susceptibility of superconductor films, such as a magnetic moment that is independent of film thickness and the variation of susceptibility with angle, are related to demagnetization. Demagnetizing factors of superconductor cylinders are significantly different from those commonly tabulated for materials with small susceptibilities. Rules for the susceptibility of mixtures with specific demagnetizing factors are used to estimate the volume fraction of superconducting grains in sintered materials. Common misunderstandings of the Meissner effect, magnetic units, and formula conversions are discussed. There is a comprehensive summary of critical-state formulas for slabs and cylinders, including new equations for complex susceptibility in large alternating fields. Limitations on the use of the critical-state model for deducing critical current density are listed and the meaning of the imaginary part of susceptibility is considered.</p>			
12. KEY WORDS (6 TO 12 ENTRIES; ALPHABETICAL ORDER; CAPITALIZE ONLY PROPER NAMES; AND SEPARATE KEY WORDS BY SEMICOLONS)  calibrations; critical current; critical field; critical-state model; critical temperature; demagnetization; demagnetizing factors; granular superconductors; intergranular coupling; Meissner effect; susceptibility; susceptometers; superconductors; thick films.			
13. AVAILABILITY		14. NUMBER OF PRINTED PAGES	
<input checked="" type="checkbox"/> UNLIMITED <input type="checkbox"/> FOR OFFICIAL DISTRIBUTION. DO NOT RELEASE TO NATIONAL TECHNICAL INFORMATION SERVICE (NTIS). <input type="checkbox"/> ORDER FROM SUPERINTENDENT OF DOCUMENTS, U.S. GOVERNMENT PRINTING OFFICE, WASHINGTON, DC 20402. <input checked="" type="checkbox"/> ORDER FROM NATIONAL TECHNICAL INFORMATION SERVICE (NTIS), SPRINGFIELD, VA 22161.		36	
		15. PRICE	

ELECTRONIC FORM





